Available online at www.sciencedirect.com
ScienceDirect
Developmental Biology 306 (2007) 94–111
DEVELOPMENTAL BIOLOGY
www.elsevier.com/locate/ydbio

Wingless/Wnt signal transduction requires distinct initiation and amplification steps that both depend on Arrow/LRP

Shahana Baig-Lewis, Wynne Peterson-Nedry, Marcel Wehrli *

Oregon Health and Science University, Department of Cell and Developmental Biology, 3181 SW Sam Jackson Park Road/L215, Portland, OR 97239, USA

Received for publication 13 July 2006; revised 1 March 2007; accepted 5 March 2007
Available online 13 March 2007

Abstract

Members of the Wg/Wnt family provide key intercellular signals during embryonic development and in the maintenance of homeostatic processes, but critical aspects of their signal transduction pathways remain controversial. We have found that canonical Wg signaling in *Drosophila* involves distinct initiation and amplification steps, both of which require Arrow/LRP. Expressing a chimeric Frizzled2-Arrow protein in flies that lack endogenous Wg or Arrow showed that this construct functions as an activated Wg receptor but is deficient in signal amplification. In contrast, a chimeric Arrow protein containing the dimerization domain of Torso acted as a potent amplifier of Wg signaling but could not initiate Wg signaling on its own. The two chimeric proteins synergized, so that their co-expression largely reconstituted the signaling levels achieved by expressing Wg itself. The amplification function of Arrow/LRP appears to be particularly important for long-range signaling, and may reflect a general mechanism for potentiating signals in the shallow part of a morphogen gradient.

Keywords: Wnt signaling; Wingless; Arrow; LRP; Frizzled; Axin; Signal amplification; Morphogen gradient

Introduction

Secreted glycoproteins of the Wingless (Wg)/Wnt family provide key signals during development and also contribute to a variety of homeostatic processes that regulate growth in adult tissues (reviewed in Logan and Nusse, 2004). Dysregulation of Wnt signaling results in severe embryonic defects and can exacerbate several types of neoplasm, including colorectal cancer, leukemia and medulloblastoma (Reya and Clevers, 2005). Despite numerous studies into the role of Wnts in both normal and abnormal contexts, however, critical aspects of the mechanisms of Wnt signaling remain poorly understood.

Wnt signals can activate three distinct pathways: planar polarity signaling, Ca^{2+}-mediated signaling, and 'canonical' Wnt signaling (reviewed in Veeman et al., 2003). Key to the execution of canonical Wnt signaling is the stabilization of β-catenin (*Drosophila* Armadillo, Arm). In response to secreted Wnts, the Wnt receptors of the Frizzled family (Fz) initiate a cytoplasmic signaling cascade that ultimately inhibits the degradation of β-catenin, which in turn results in β-catenin-mediated regulation of gene expression (Behrens et al., 1996; Funayama et al., 1995; Logan and Nusse, 2004; Orsulic and Peifer, 1996). Previous studies have indicated that Wnt signaling acts by inhibiting a β-catenin destruction complex containing APC, the scaffold protein Axin, and the serine/threonine kinase GSK-3β (*Drosophila* Zeste-white3, Zw3). In the absence of Wnt, the Axin complex binds β-catenin/Arm, while prior phosphorylation of Arm by CK1α primes its subsequent phosphorylation by GSK3β/Zw3. This second phosphorylation step provides the signal for β-catenin ubiquitination and degradation by the proteasome. Precisely how Wnt signaling prevents β-catenin/Arm phosphorylation by the destruction complex remains ambiguous, though Dishevelled (Dvl; *Drosophila*, Dsh) appears to be a key mediator of this inhibition.

It is well established that members of the Frizzled family of serpentine proteins bind Wnt ligands and are necessary for transducing Wnt signals (Logan and Nusse, 2004). Frizzled subunits bind Dishevelled at a site essential for Wnt signaling (Cong et al., 2004; Wong et al., 2003), while deletion of functionally redundant Frizzled receptors eliminates Wnt

* Corresponding author.
E-mail address: wehrlim@ohsu.edu (M. Wehrli).

0012-1606/$ - see front matter © 2007 Elsevier Inc. All rights reserved.
doi:10.1016/j.ydbio.2007.03.005

signaling (Chen and Struhl, 1999; Kennerdell and Carthew, 1998). Besides Frizzled receptors, a subfamily of low-density lipoprotein (LDL)-receptor-related proteins (LRPs), consisting of mammalian LRP5 and 6 and *Drosophila* Arrow, function as co-receptors for Wnts (Kelly et al., 2004; Pinson et al., 2000; Tamai et al., 2000; Wehrli et al., 2000). Genetic evidence from *Drosophila* demonstrates that Arrow is absolutely essential for signal transduction downstream of the *Drosophila* Wnt ligand, Wingless (Wg). Specifically, over-expression of Wg ligand cannot compensate for the loss of Arrow, while expression of Dsh can still activate the intracellular cascade in this context. Mosaic analysis has also suggested that Arrow/LRP function is required by the signal-receiving cell rather than by the cell that dispatches Wg/Wnt (Tamai et al., 2000; Wehrli et al., 2000). Furthermore, physical proximity between the intracellular domain of Arrow and the Frizzled 2 receptor (Fz2) is critical for the initiation of Wg signaling at the membrane: a Fz2-Arr fusion protein that mimics the normal proximity of these proteins is sufficient to trigger the Wg signaling cascade in vivo in the absence of either Wg ligand or Frizzled receptors, and it largely compensates for the loss of endogenous Arrow (Fig. 1; Tolwinski et al., 2003). Thus, Arrow (as well as its vertebrate homologues) appears to be essential components of functional Wnt receptors.

Precisely how the Wg receptor complex initiates the cytoplasmic cascade that is required for Wg signaling remains elusive. Both Arrow and LRP5 and 6 can associate with Axin, suggesting that these interactions may provide a mechanism for inhibiting the β-catenin destruction complex (Mao et al., 2001; Tolwinski et al., 2003). However, the Axin–Arr/LRP interaction is secondary to the initiation of the Wg signal and requires Dsh function, which promotes the translocation of Axin to the cell membrane (Cliffe et al., 2003; Mao et al., 2001). In addition, our previous studies suggested that Arrow not only plays an essential role as a Wg co-receptor, but also may function downstream of signal initiation to amplify the initial Wg signal (Tolwinski et al., 2003; Wehrli et al., 2000). Specifically, we found that chimeric Fz2-Arr receptors containing the intracellular portion of Arrow rescue *wingless*$^-$ mutant embryos (which also express endogenous Arrow) more completely than it rescues *arrow*$^-$ mutants (which do not; Figs. 1B, C). One interpretation of this observation is that Arrow functions as a co-receptor with Fz2 for signal initiation, and that Fz2-Arr can independently fulfill this role in either a *wingless*$^-$ or *arrow*$^-$ mutant. However, the inability of Fz2-Arr to fully rescue an *arrow*$^-$ mutant also suggests that Arrow serves a second downstream function that is independent of Fz2 activation. The ability of wild-type, endogenous Arrow to perform this function may reflect a requirement for information contained in the transmembrane or extracellular portions of Arrow, neither of which were included in our original Fz2-Arr chimeric receptors. Wg signaling may therefore involve a two-step process: signal initiation, which is mediated by Frizzled/Arrow co-receptor complexes, and signal amplification, which also requires Arrow but may be independent of Frizzled.

To test this hypothesis, we have generated several new Arrow-derived constructs to probe the molecular interactions underlying Wg signaling in vivo. In particular, we created an extracellularly truncated, dimerizing version of Arrow (tor^{D}Arr) that greatly potentiates Wg signaling, and a corresponding non-dimerizing construct (tor^{WT}Arr), which does not effectively potentiate Wg signaling. In the current study, we have compared the ability of these constructs to rescue Wg signaling in different developmental contexts, which has allowed us to distinguish the role of these proteins in Wg signal initiation versus signal amplification. Notably, our experiments indicate that these two steps occur sequentially, but that both require Arrow. These results provide new insight into the role of Arrow/LRP in mediating Wg signaling; they also suggest that this type of signal amplification may represent a general principle by which cells detect low levels of diffusible molecules, such as may occur in the shallow part of a long-range morphogen gradient.

Results

A dimerizing, extracellularly truncated version of Arrow potentiates Wg signaling

During the normal process of segmentation in *Drosophila* embryos, Wg signaling is required for the establishment of alternating bands of smooth cuticle and bands of hook-like protrusions, called denticles (Babu, 1977; Nüsslein-Volhard and Wieschaus, 1980). If the Wg pathway is disrupted (e.g., in *wingless*$^-$ or *arrow*$^-$ mutant embryos), no smooth cuticle is formed, and instead embryos display a lawn of denticles. We previously showed that our Fz2-Arr chimera functions as a constitutively active Wg receptor capable of stimulating the Wg signaling cascade in the absence of Wg ligand (Tolwinski et al., 2003). However, when we compared the extent of smooth cuticle rescued by Fz2-Arr in embryos lacking Arrow versus embryos lacking Wingless (but wild type for Arrow), we found a more complete rescue in the *wingless*$^-$ mutants (Figs. 1B, C; 30 °C). In *wingless*$^-$ embryos, expressing Fz-Arr in every other segment provided the maximal level of rescue, manifested by 4 smooth cuticle bands in the abdominal region (Fig. 1B; 30 °C). In contrast, expression of Fz-Arr in *arrow*$^-$ embryos produced only a partial rescue, creating 1 or 2 smooth cuticle bands in the abdomen (Fig. 1C; 30 °C).

One possible explanation for this unexpected difference is that expressing Fz2-Arr in the absence of endogenous Arrow results in only a partial activation of the Wg signaling cascade, while the presence of endogenous Arrow in *wingless*$^-$ mutants provides a means of amplifying the signal generated by Fz2-Arr, resulting in a more complete rescue. Alternatively, the loss of Wingless ligand might indirectly result in greater activity or stability of Fz2-Arr. We therefore tested the effects of expressing Fz2-Arr in embryos lacking the redundant receptors Fz and Fz2 (*fz*$^-$ *fz2*$^-$), as an alternative means of disrupting the Wg pathway. As in *wingless*$^-$ embryos, expressing the Fz2-Arr construct in *fz*$^-$ *fz2*$^-$ mutants produced embryos with 4 smooth abdominal cuticle bands (Fig. 1D; 30 °C). This result is consistent with previous studies in which we used engrailed-Gal4 to drive Fz2-Arr expression (Tolwinski et al., 2003), supporting the model that the presence of Arrow in *wingless*$^-$

and *fz*⁻ *fz2*⁻ embryos is capable of potentiating the Fz2-Arr signal, whereas it cannot do so in *arrow*⁻ embryos.

We then asked whether the stability of the Fz2-Arr construct might be different in *wingless*⁻ versus *arrow*⁻ embryos, as a possible explanation for the difference in signaling that we documented in these two mutant lines. Taking advantage of the 6x-myc-tag present in Fz2-Arr (Fig. 1A), we immunostained *wingless*⁻ and *arrow*⁻ null mutant embryos with anti-myc antibodies (Figs. 1G, H; 30 °C; Materials and methods). After background subtraction, the averaged mean values for relative fluorescence of Fz2-Arr stripes are 12.5±6.6 (n=26) for *wingless*⁻ and 22.0±5.5 (n=20) for *arrow*⁻ embryos. Since these values are not significantly different, we conclude that differential Fz2-Arr protein stability does not account for the increased level of Wg signaling that is induced by Fz2-Arr in *wingless*⁻ and *fz*⁻ *fz2*⁻ mutant embryos, as compared to the effects of Fz2-Arr in *arrow* null mutants (Figs. 1B–D).

An unexpected feature revealed by these studies was that Fz2-Arr produces a graded rescue of smooth cuticle banding in the anterioposterior direction (Figs. 1B and C). We speculated that this effect might be due either to the graded expression of the prd-Gal4 driver or might be the manifestation of an as yet

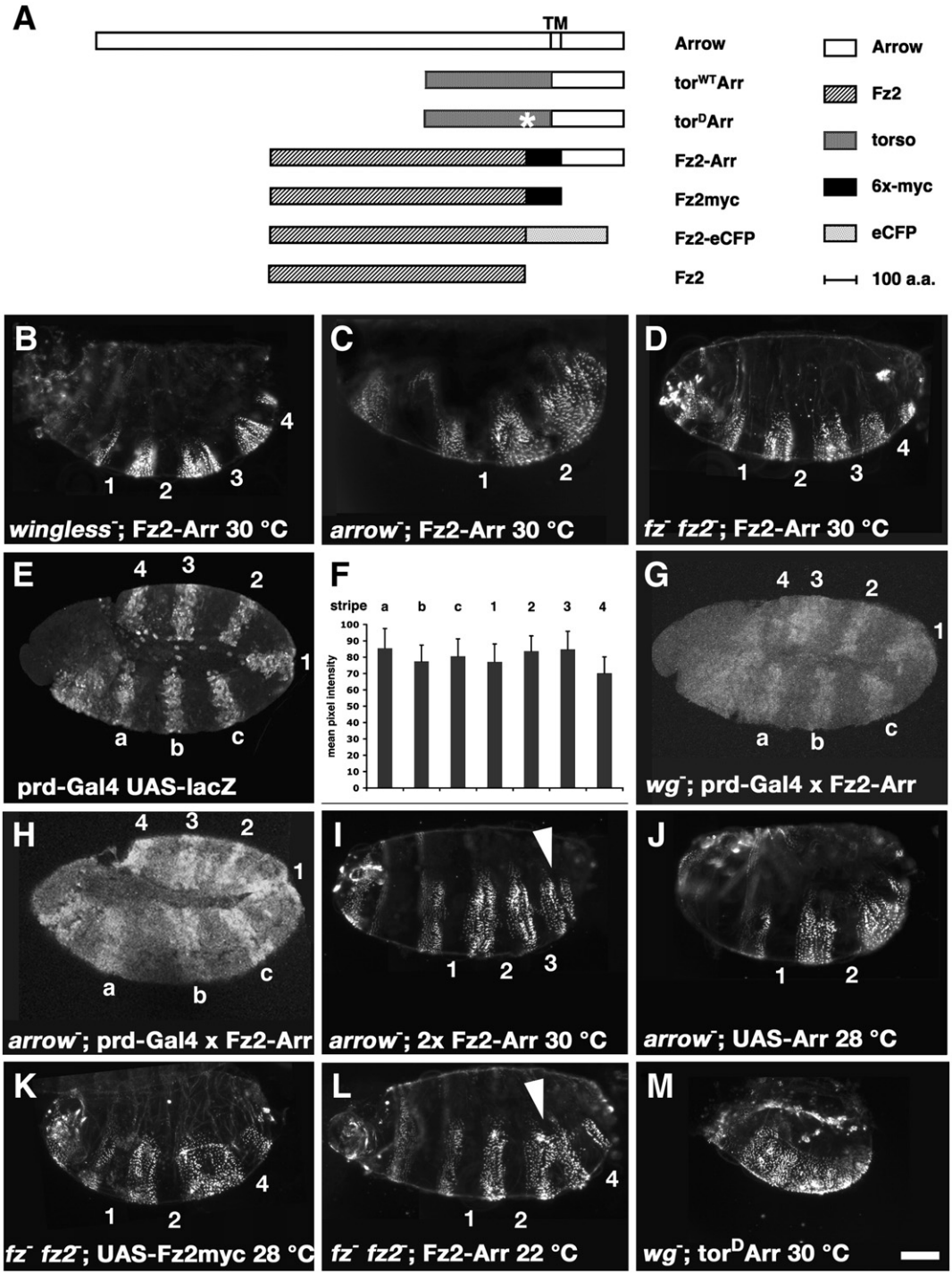

unknown graded requirement for Wg signaling. To test for graded changes in prd-Gal4 expression, we drove UAS-lacZ expression with prd-Gal4, immunostained the embryos with anti-lacZ, and quantified the average fluorescence intensity of each stripe (Figs. 1E, F; Materials and methods). Besides some minor variation between individual stripes within an embryo or between embryos, we found no evidence for an anterioposterior gradient of prd-Gal4-driven expression. Instead, this result suggests that a graded requirement for Wg signaling may play a role in the anterioposterior patterning of the embryonic cuticle.

We hypothesized that if such a graded requirement of Wg signaling resulted in the need for higher levels of signal for normal development posteriorly, then the defects seen in *arrow* mutants should be rescued by an increase in Fz2-Arr expression levels. Alternatively if development in the posterior embryonic region involves qualitatively different properties for Wg signaling than in the anterior regions, then higher levels of Fz2-Arr would still not result in the generation of smooth cuticle formation in the posterior domain. Expressing 2× Fz2-Arr (30 °C) in *arrow* mutant embryos results in the generation of a third, almost complete band of smooth cuticle and a very narrow, incomplete fourth band (Fig. 1I, arrowhead). Though the extent of rescue still falls short of full rescue (compare to Figs. 1B, C), this result suggests that the posterior regions of *arrow* null mutants can nevertheless respond to increased signaling by Fz2-Arr, arguing against qualitatively different Wg signaling requirements in the anterior versus posterior domains.

The foregoing result also suggests that a graded increase in Wg signaling is normally required in the posterior embryo, and that a greater than 2-fold increase is needed compared to the anterior region. Such a model predicts that signaling levels should also first fall below a threshold in the posterior regions of embryos that express limiting amounts of Arrow or Frizzleds. To test this idea, we took advantage of the temperature sensitivity of Gal4 activity (which in flies is maximal at 30 °C and minimal at 16 °C) to express limiting amounts of Arrow in *arrow* null mutants (Fig. 1J; 28 °C). We previously showed that expression of Arrow at 30 °C generates four smooth cuticle bands in the abdomen, though the rescue is not complete (Wehrli et al., 2000, and data not shown). In contrast, expressing Arrow at 28 °C results in the loss of two bands of smooth cuticle (Fig. 1J). These findings demonstrate an increased requirement for Arrow and Wg signal transduction posteriorly. They also suggest that the maximal levels of Arrow expression obtained with the prd-Gal4 driver at 30 °C in *arrow* null mutants fails to reach the high levels present in wild-type animals, particularly the large amount of Arrow provided by maternal contribution (M.W., unpublished observation).

Using this same experimental strategy, we next analyzed the effects of expressing limiting levels of Fz2 (Fz2myc) in fz^{-} $fz2^{-}$ mutant embryos. When we performed this experiment at 30 °C (for maximal Gal4 activity), we found that Fz2myc can fully rescue patterning defects in fz^{-} $fz2^{-}$ mutants (not shown). In contrast, expressing lower Fz2 levels (at 28 °C) results in only a partial rescue, manifested by the loss of one smooth cuticle band (Fig. 1K; in this embryo, the 3rd band is missing). Therefore, limited expression of either Arrow or Fz2 results in the pronounced loss of posterior smooth cuticle, equivalent to what we observed in our initial expression of Fz2-Arr in *arrow* null mutants (Fig. 1C; 30 °C).

Given our observation that the patterning defects seen in fz^{-} $fz2^{-}$ mutants could be fully rescued by expressing either Fz2-Arr (at 30 °C; Fig. 1D) or Fz2 itself (not shown), we asked whether this rescue effect is simply due to the Fz2 part of the Fz2-Arr fusion protein or whether this construct increases Wg signaling by functioning as an activated receptor (as suggested by our experiments using *wingless* and *arrow* mutants; Tolwinski et al., 2003; Figs. 1B, C). By expressing Fz2-Arr in fz^{-} $fz2^{-}$ mutant embryos at increasingly lower temperatures (to titrate down Fz2-Arr levels), we found that embryos grown at 22 °C exhibited a mild reduction in

Fig. 1. A graded requirement for Wg signaling in the anterior–posterior axis of developing embryos. (A) Schematic representation of constructs used in this study. The transmembrane domain (TM) is indicated for Arrow; * denotes the Y327C mutation that renders Torso dominant. UAS-Arr is from Wehrli et al. (2000); UAS-Fz2-Arr, UAS-Fz2myc, Fz2-eCFP are from Tolwinski et al. (2003), UAS-tor^{WT}Arr and tor^{D}Arr are described in this study. (B–M) In all of these panels, prd-Gal4 was used to drive construct expression, while the temperature dependence of Gal4 activity was used to vary expression levels. (B–D, I–M) dark-field illumination of embryonic cuticles. (B) In a *wingless*^{null} mutant embryo, driving expression of Fz2-Arr with prd-Gal4 generates four bands of smooth cuticle, signifying a full rescue. (C) Using the same expression system in an *arrow*^{null} embryo, only a partial rescue is observed. (D) In a fz^{-} $fz2^{-}$ embryo, Fz2-Arr expression provides full rescue. (E) prd-Gal4-driven UAS-lacZ in a stage 10 embryo (30 °C) is visualized by immunostaining and detected by confocal microscopy. The posterior four bands of prd-Gal4 expression (numbered 1–4) in the abdominal region are responsible for generating the smooth cuticle bands induced by Fz2-Arr expression (shown in panels B and D; also numbered 1–4). All stripes of lacZ expression show similar intensities. (F) prd-Gal4-driven lacZ expression in stage 10 embryos (see panel E) was quantified as average fluorescence within a stripe. Average fluorescence between corresponding stripes of different embryos was then compared (error bars indicate standard deviations). No graded expression is detected in the anterioposterior direction. (G) prd-Gal4-driven Fz2-Arr expression (30 °C) visualized by immunofluorescence in a *wg*^{null} embryo, using the 6x-myc tag present in Fz2-Arr (detected with anti-myc antibodies). All stripes express similar levels of Fz2-Arr, which are statistically indistinguishable from expression levels seen in *arr*^{null} mutants (H, and see text). (H) *arr*^{null} mutant embryo expressing Fz2-Arr with prd-Gal4 (30 °C) and visualized as in panel G. Similar levels of Fz2-Arr expression are detected in the stripes of these animals, which are comparable to expression levels detected in *wg*^{null} embryos (see text). (I) Expression of two copies of Fz2-Arr generates 3 bands of abdominal smooth cuticle (#3 is incompletely separated); a very narrow and incomplete 4th band of smooth cuticle is also visible (arrowhead). Rescue is clearly enhanced by the higher dosage of Fz2-Arr (compare with panel C). (J) Limiting the expression of UAS-Arr in an *arr*^{null} mutant embryo (28 °C) results in a partial rescue (an anterior versus posterior difference is apparent; compare with the rescue patterns seen in panels C and I). (K) Limiting the expression of Fz2myc in a fz^{-} $fz2^{-}$ embryo shows also loss of rescue in the posterior rather then anterior region of the embryo (similar to panel J). (L) Partial rescue of fz^{-} $fz2^{-}$ embryo with expression of Fz2-Arr is apparent from the incomplete formation of smooth cuticle band #3 (arrowhead), but occurs only when expression levels are severely reduced (at 22 °C), compared to Fz2 expression at 28 °C (K). (M) Maximal expression of tor^{D}Arr in *wg*$^{-}$ induces no smooth cuticle. Scale bar=40 μm (B–E, G–M). Data in panels B and C were previously presented in Tolwinski et al., 2003 and are included here for comparison.

rescue, manifested as partial loss of smooth cuticle (Fig. 1L, compare to Fig. 1D). If the actual level of signaling in Figs. 1K and L is considered roughly equivalent, based on cuticle phenotype, then the much lower expression levels of Fz2-Arr at 22 °C (Fig. 1L) must be overcome by higher signaling activity, compared to Fz2 alone (Fig. 1K; 28 °C). These results provide additional support for our model that Fz2-Arr functions as an activated receptor, whether expressed in *wingless* mutants, *arrow* mutants, or *fz*$^{-}$ *fz2*$^{-}$ mutant embryos.

As in our earlier studies, these preparations also revealed a graded requirement for Wg signaling in embryos, whereby increased Wg signaling is required more posteriorly. By limiting the expression levels of Fz2-Arr, we created a sensitized situation (in the posterior but not anterior regions), demonstrating that similar levels of Fz2-Arr induced a lower level of Wg signaling in *arrow*$^{-}$ mutants than in embryos expressing endogenous Arrow protein (*wingless*$^{-}$ or *fz*$^{-}$ *fz2*$^{-}$). These results indicate that wild-type Arrow might serve a secondary function during Wg signaling, resulting in the amplification of the signal initiated by ligand–receptor interactions. The nature of this graded Wg signaling requirement remains to be elucidated; however, it could potentially result from limited processing of a pathway component, as has been suggested for graded Notch signaling in mouse embryos (Huppert et al., 2000).

We were thus interested in how Arrow might potentiate Wg signaling after its initiation. Receptor clustering promotes signaling in other pathways (e.g., RTK, Dickson et al., 1992; Dpp, Nellen et al., 1996; integrin, Werb et al., 1989), and previous studies in cell culture have indicated that dimerization of LRP6 (a vertebrate orthologue of Arrow) potentiates its signaling capacity (Cong et al., 2004). We therefore tested whether dimerization of the Arrow intracellular domain would also induce a detectable response. To this end, we removed the extracellular domain of Arrow and replaced it with the extracellular domain of the *Drosophila* tyrosine kinase Torso (*tor*), creating tor^{WT}Arr; this control construct should not induce dimerization. Alternatively, we used a constitutively dimerizing form of Torso to create tor^{D}Arr, a strategy that has previously been used to induce dimerization of fusion proteins (Dickson et al., 1992) (Fig. 1A). In a wild-type embryo, denticles are of characteristic size and orientation (Fig. 2A), and their formation requires subthreshold Wg signaling. When we expressed tor^{D}Arr in a wild-type embryo using the ptc-Gal4 driver, several rows of denticles were re-specified to form smooth cuticle (Fig. 2B), while expression of tor^{WT}Arr had no effect on denticle fate (not

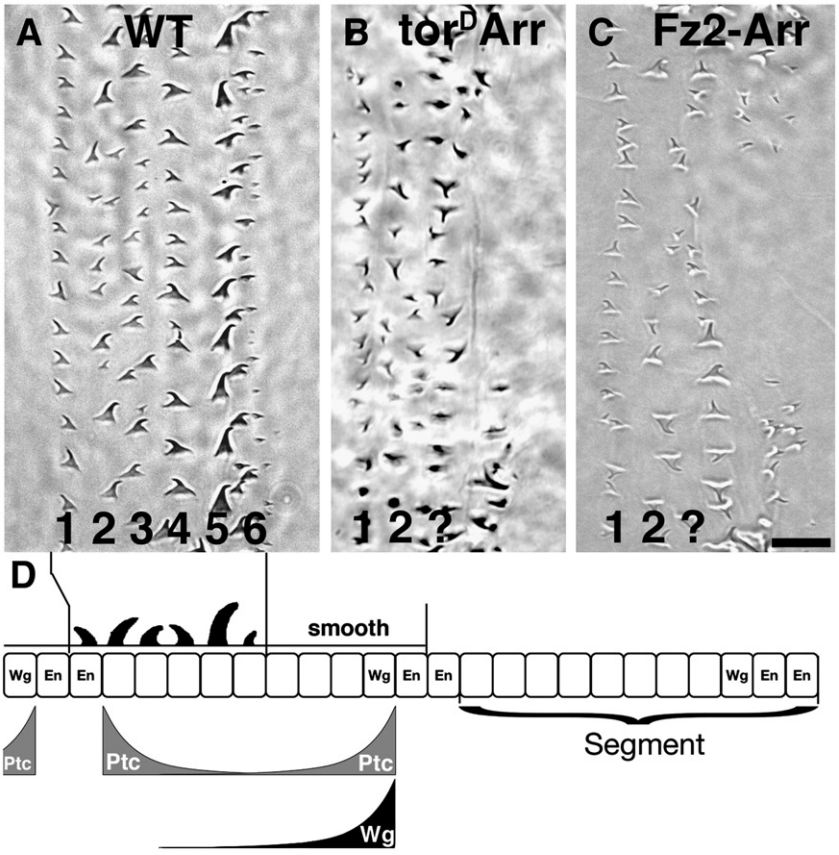

Fig. 2. tor^{D}Arr potentiates Wg signaling in the embryo and expands smooth cuticle fate. (A) In wild-type embryos (wt), six rows of denticles differentiate with characteristic denticle orientation and shapes. (B) tor^{D}Arr expressed with ptc-Gal4 causes the loss of several rows of posterior denticles (rows 3–6). (C) Expression of Fz2-Arr under the control of ptc-Gal4 re-specifies these posterior denticles as smooth cuticle (data from Tolwinski et al., 2003). In panels A–C, only part of the smooth cuticle territory is shown. (D) Schematic diagram showing the expression domains for Ptc and Wg in two adjacent segments of embryonic cuticle (modified from Hatini and DiNardo, 2001). Ptc is induced by Hedgehog, which is produced by Engrailed (En) cells; Wg ligand is rapidly degraded in En cells resulting in an asymmetric Wg gradient (Dubois et al., 2001). Scale bar = 10 μm (A–C).

shown). This finding is consistent with an amplification of the Wg signaling gradient by tor^{D}Arr in regions of cuticle that normally produce denticles, thereby altering the specification of these regions to a smooth cuticle fate. They also indicate that this amplification step may normally require Arrow dimerization.

tor^{D}Arr cannot initiate Wg signaling in the absence of Wg ligand or receptors

In previous work, we found that the expression of Fz2-Arr also induced the differentiation of smooth cuticle (a hallmark of Wg signaling), in that it abolished the expression of posterior rows of denticles (Tolwinski et al., 2003; see Fig. 2D). These studies also established that Fz2-Arr could activate the Wg signaling pathway independent of Wg ligand: Fz2-Arr restored signaling in *wg^{null}* or *fz^{null} fz2^{null}* mutant embryos, although no signaling was observed if the downstream components Dishevelled or Armadillo were removed (Fig. 3; the left panel graphically represents the results of our previous work for comparison). However, while Fz2-Arr could stimulate the endogenous Wg signaling pathway independent of Wg, it provided only partial rescue in the absence of endogenous Arrow (Figs. 1C and 3), providing the first hint that Arrow must participate in an additional step in the Wg signaling pathway (Tolwinski et al., 2003).

Given our observation that tor^{D}Arr expression can also modulate denticle fate (Fig. 2B), we hypothesized that this construct might also induce Wg signaling in the absence of ligand. We therefore tested its ability to rescue Wg signaling in the absence of endogenous Wg. In contrast to Fz2-Arr, however, no smooth cuticle was ever observed when we expressed tor^{D}Arr at maximal levels (30 °C) in alternating segments within *wg^{null}* embryos (Fig. 1M), nor was Wg signaling activated by this construct in any of the other genotypes that we tested, including *fz^{null} fz2^{null}*, *arr^{null}*, *dsh^{null}*, or *arm^{strong}* (Fig. 3 middle panel; for the details of these crosses, see Materials and methods). These results indicate that tor^{D}Arr activity is Wg-dependent and requires an intact Wg signaling pathway to exert its effect. Thus, in contrast to Fz2-Arr, which can initiate a signal *de novo*, tor^{D}Arr can only amplify a signal that has already been initiated by the Wg receptor. These results indicate that tor^{D}Arr does not function as an activated receptor. We also tested the possibility that dimerization might block the activity of tor^{D}Arr by expressing a construct containing the wild-type Torso domain, tor^{WT}Arr (Fig. 1A). However, we also failed to detect smooth cuticle in any of the genotypes tested (*wg^{null}*, *fz^{H51} fz2^{C1}*, *arr^{null}*; Fig. 3, right panel). Taken together, our data suggest that tor^{D}Arr can potentiate Wg signaling but cannot initiate a signal in the absence of Wg ligand or any of the pathway components required for Wg signal initiation or transduction (Arrow, Frizzleds, Dsh, Arm).

tor^{D}Arr synergizes with Fz2-Arr in the embryo

Based on the foregoing observations that tor^{D}Arr requires an intact Wg signaling pathway to exert its effects on cuticle fate, we next tested whether tor^{D}Arr might also be able to amplify a signal generated by Fz2-Arr. Such an effect would lend further support for our model that Arrow serves a second, amplifying function once Wg signaling has been initiated. To test for synergy between Fz2-Arr and tor^{D}Arr, we took advantage of our sensitized assay for Wg signaling by reducing the level of Fz2-Arr, which results in an incomplete rescue of the smooth

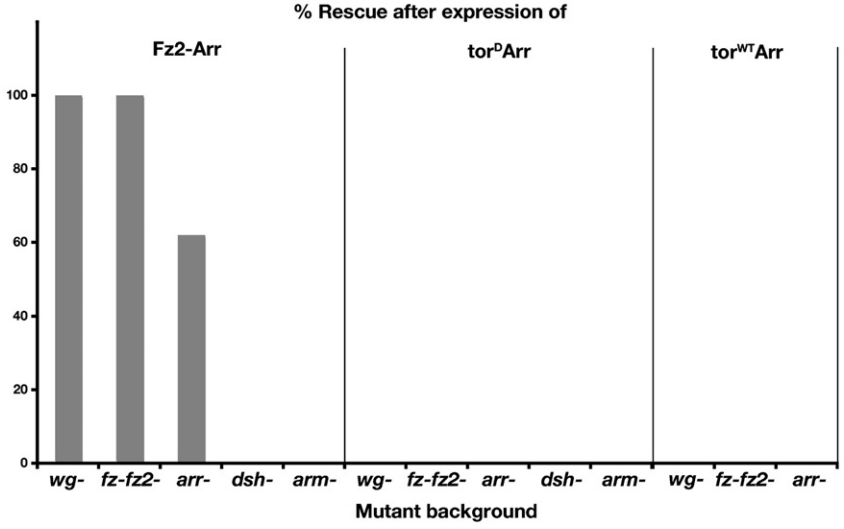

Fig. 3. tor^{D}Arr activity requires an existing Wg signal. As summarized in the left panel, Fz2-Arr expressed in the prd-Gal4 pattern fully rescues smooth cuticle in the absence of either Wg or the Frizzleds (*fz^{-} fz2^{-}*), and substantially rescues smooth cuticle in the absence of Arrow. However, Fz2-Arr signaling critically depends on Dishevelled and Armadillo (data shown previously in Tolwinski et al., 2003). In contrast, expression of tor^{D}Arr expressed in the prd-Gal4 pattern fails to rescue smooth cuticle in the absence of any of the Wg pathway components tested (middle panel). Mutants tested and number of embryos (rescued/not rescued) are as follows: *wg^{CX4}* 0/163; *fz^{H51} fz2^{C1}* 0/137; *arr^{2}* 0/258; *dsh^{V26}* 0/283; *arm^{XM19}* 0/88. Expression of tor^{WT}Arr with prd-Gal4 also fails to generate smooth cuticle (right panel); *wg^{CX4}* 0/172; *fz^{H51} fz2^{C1}* 0/72; *arr^{2}* 0/67 ($P < 10^{-4}$ or better in χ^2 analysis; in these experiments, 25% of embryos are of the genotype that could potentially display rescue).

cuticle phenotype (as described above). Driving Fz2-Arr expression with prd-Gal4 at 30 °C fully rescued signaling, even in the absence of Wg ligand (compare Figs. 4A and B). However, if Gal4 activity was reduced by lowering the temperature to 25 °C, Fz2-Arr-dependent signaling was only partially rescued (Fig. 4C). In this sensitized situation, co-expression of tor^{D}Arr significantly increased the frequency of full rescue, as manifested by its ability to provide maximal rescue of smooth cuticle in the prd-Gal4 pattern (Figs. 4D, E; $P < 0.0001$). In contrast, co-expression of Fz2-Arr with either tor^{WT}Arr, additional wild-type Arrow, or Fz2-CFP (Fz2 tagged with cyan fluorescent protein, CFP; Fig. 1A) failed to significantly increase the signaling attained by Fz2-Arr alone (Fig. 4E), again indicating that Arrow dimerization is required for this effect. The observed synergy of Fz2-Arr + tor^{D}Arr also showed that tor^{D}Arr could amplify a signal initiated by Fz2-Arr

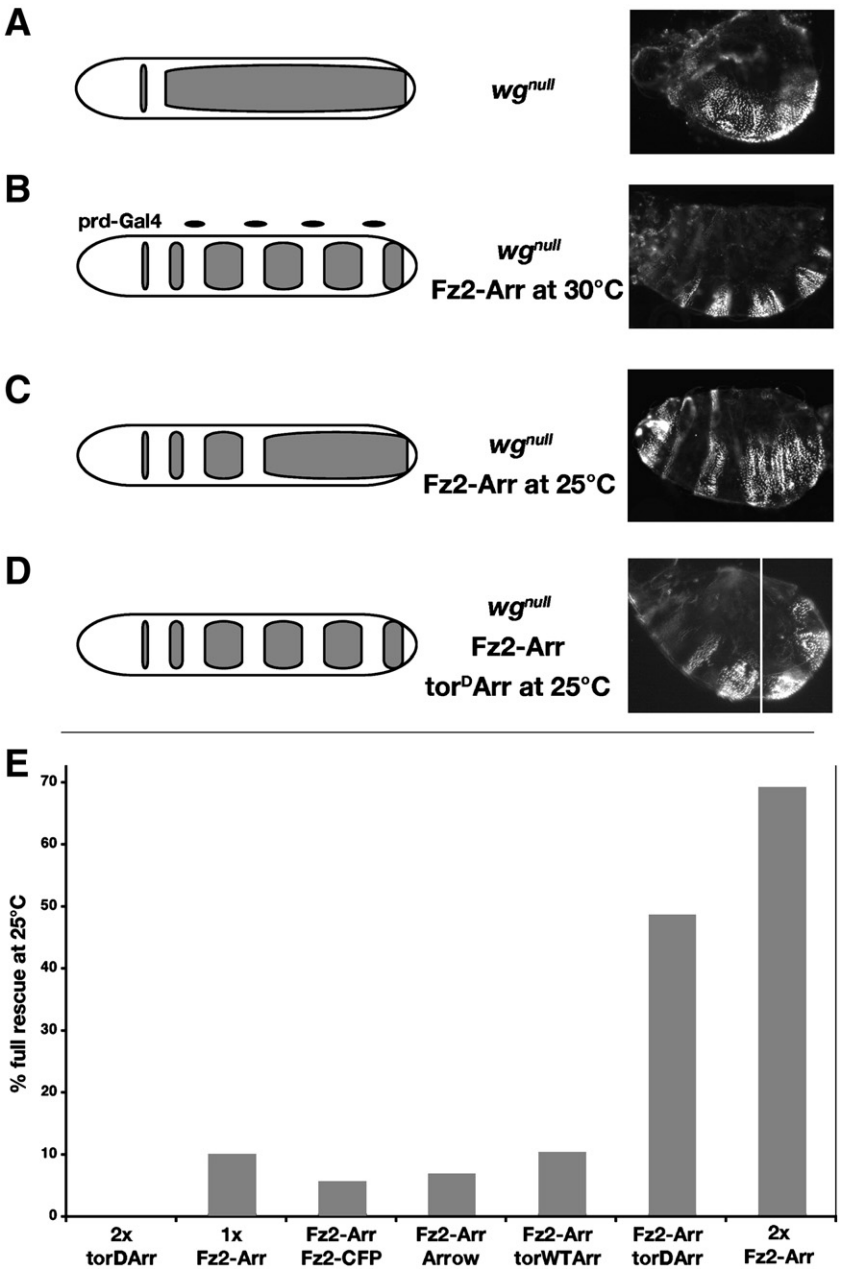

Fig. 4. Fz2-Arr and tor^{D}Arr synergize to restore Wg signaling in the embryo. Panels A–D show schematic diagrams and representative preparations of each manipulation. (A) A *wingless*^{null} mutant is devoid of smooth cuticle. (B) In *wingless*^{null} mutants raised at 30 °C (to maximize Gal4 activity), prd-Gal4 drives expression of Fz2-Arr in alternate segments, providing maximal rescue (see also Tolwinski et al., 2003). (C) When these animals are raised at 25 °C to reduce Gal4 transcriptional activity and Fz2-Arr levels, incomplete rescue ensues. (D) Introducing tor^{D}Arr in such an embryo restores full rescue. Such embryos are frequently curled; the right panel shows two focal planes to reveal all four abdominal smooth cuticle bands. (E) Quantification of the ability of different combinations of our chimeric constructs to potentiate signaling and fully rescue the genotype shown in panel C. No signaling was detected with 2× tor^{D}Arr alone (see also Fig. 2); 1× Fz2-Arr results in full rescue 10% of the time (4/40), and no significant increase is detected by co-expression of Fz2-Arr with Fz2-CFP (5/88), Arrow (2/29), or tor^{WT}Arr (8/77) ($P < 0.0001$). A significant increase in signaling is only observed upon co-expression of tor^{D}Arr (17/35) or a second copy of Fz2-Arr (36/52) ($P < 0.0001$).

even in the absence of endogenous Wg ligand (Fig. 4D). Since tor^{D}Arr by itself could not initiate a signal in the absence of Wg (Fig. 3), these results support our model that besides playing an essential role in the induction of Wg signaling, Arrow also serves a second function that requires its dimerization and results in the further amplification of signals that have already been initiated.

tor^{D}Arr potentiates Wg signaling in the developing wing

Our studies in developing embryos revealed a profound difference between the effects of our two chimeric receptor constructs: while Fz2-Arr could initiate a signal de novo, tor^{D}Arr could only exert an effect in the presence of an activated Wg signaling pathway. These results support the model that the two constructs mimic two distinct steps during Wg signaling: Fz2-Arr mimics signal initiation by the endogenous receptor complex (consisting of Arrow and Frizzleds) in response to Wg ligands, while tor^{D}Arr exclusively mimics the amplification of an activated Wg signal (a process that requires Arrow dimerization; see also Figs. 1B, C). Since this type of signal amplification by Arrow might be more apparent in situations requiring long-range signaling, we next directed our attention to the fly wing, where Wg functions as a long-range morphogen (Couso et al., 1993; Neumann and Cohen, 1997; Zecca et al., 1996).

Wing margin bristles are a Wg-dependent cell type that forms in response to the highest levels of Wg protein, which are normally found near the dorsoventral (D/V) boundary in the wing imaginal disc (the region that later becomes the wing margin). Previous studies have shown that manipulations designed to increase the level of Wg signaling in the wing disc cause ectopic bristles to form in a wider area of the wing around the margin (Axelrod et al., 1996; Cadigan et al., 1998; Neumann and Cohen, 1996; White et al., 1998). We therefore used this assay to test the effects of our fusion constructs on the range of Wg signaling during wing formation. For these studies, we drove ectopic protein expression using the MS1096-Gal4 driver, which has been shown to induce high levels of expression in the developing wing (Milan et al., 1998). For example, over-expressing Arrow with this driver generated a number of ectopic bristles near the wing margin (Figs. 5A, B; see also Wehrli et al., 2000).

When we used this assay to express the non-dimerizing construct tor^{WT}Arr in wild-type flies, we observed only a few ectopic bristles, comparable to the effect of over-expressing Arrow alone (compare Fig. 5B with Figs. 5C, C′). In contrast, expression of tor^{D}Arr resulted in wing blades that were almost completely covered with ectopic margin bristles (Figs. 5D, D′), indicating once again that Arrow dimerization produces a robust amplification of Wg signaling. In order to rule out potential artifacts that might be due to differences in the levels of expression or stability of our constructs, we quantified construct expression in situ on wing discs expressing Arrow, tor^{WT}Arr, or tor^{D}Arr by ratio-imaging using an anti-Arrow antibody and ubiquitously expressed GFP as an internal standard (see Materials and methods). In addition, Western blots of wing disc lysates were performed using an anti-Arrow antibody to detect Fz2-Arr, Arrow, tor^{WT}Arr, or tor^{D}Arr. As shown in Supplemental Fig. 2, these experiments showed that these proteins were expressed at comparable levels (panels A–D), with no more than two-fold variations in expression levels between different preparations (panels E–F). Taken together, these results suggest that the intracellular domain of Arrow can provide a modest amount of signal potentiation (for example, when presented as additional wild-type Arrow or as tor^{WT}Arr), while strong potentiation of endogenous Wg signaling is achieved by dimerization or clustering of the Arrow intracellular domain (using tor^{D}Arr).

We then asked whether tor^{D}Arr activity in the developing wing depends on endogenous ligand (as observed in the embryo) or whether this construct could induce bristle formation independent of Wg ligand. As demonstrated by Axelrod et al. (1996), ectopic bristles formed by ligand-dependent potentiation of Wg signaling are primarily confined to the region of the wing margin. In contrast, ligand-independent activation of Wg signaling should also allow bristles to form away from the margin in the more central regions of the wing blade. When we reduced the expression levels of tor^{D}Arr by driving its expression at 25 °C instead of 30 °C, many fewer ectopic bristles were produced, and they tended to be confined to regions near the wing margin (Figs. 5E, E′). This results supports our model that tor^{D}Arr can potentiate an endogenous Wg signal but does not initiate signaling in the absence of ligand.

Since our experiments in embryos indicated that Fz2-Arr functions as a constitutively active receptor, we also analyzed its activity in the wing. When we expressed this construct at maximal levels (30 °C), we observed a diffuse pattern of ectopic bristle formation across the wing blade (Fig. 6A, inset; Fig. 6A′), consistent with this construct acting in a Wg-independent manner. In contrast, we did not observe this pattern of ectopic bristles when we expressed Arr, Fz2-CFP or tor^{WT}Arr throughout the wing (described in more detail below). Not surprisingly, ectopic bristles tended to be more numerous at positions nearer the wing margin (Fig. 6A, arrows), which we assume is due to the combined response of endogenous Fz2 receptors and the Fz2-Arr construct in response to endogenous Wg. Thus, as in the embryo, Fz2-Arr can activate the Wg signaling pathway independent of ligand, although these results suggest that it can also respond to endogenous Wg to enhance the normal levels of Fz2-dependent signaling.

Besides the induction of ectopic bristle formation, Fz2-Arr also caused venation defects in the wing (Fig. 6A, arrowheads). This effect was most likely due to interference with EGF receptor signaling, as previously demonstrated by other manipulations that caused ectopic Wg signaling (Neumann and Cohen, 1996; White et al., 1998). When we reduced Fz2-Arr levels by driving its expression at 25 °C, the production of venation defects was also greatly reduced, and no ectopic bristles were apparent (Fig. 6C). This result suggests that the reduced levels of Fz2-Arr were not able to generate sufficient signaling independent of Wg to reach the threshold necessary for bristle determination, and only rarely exceeded the threshold

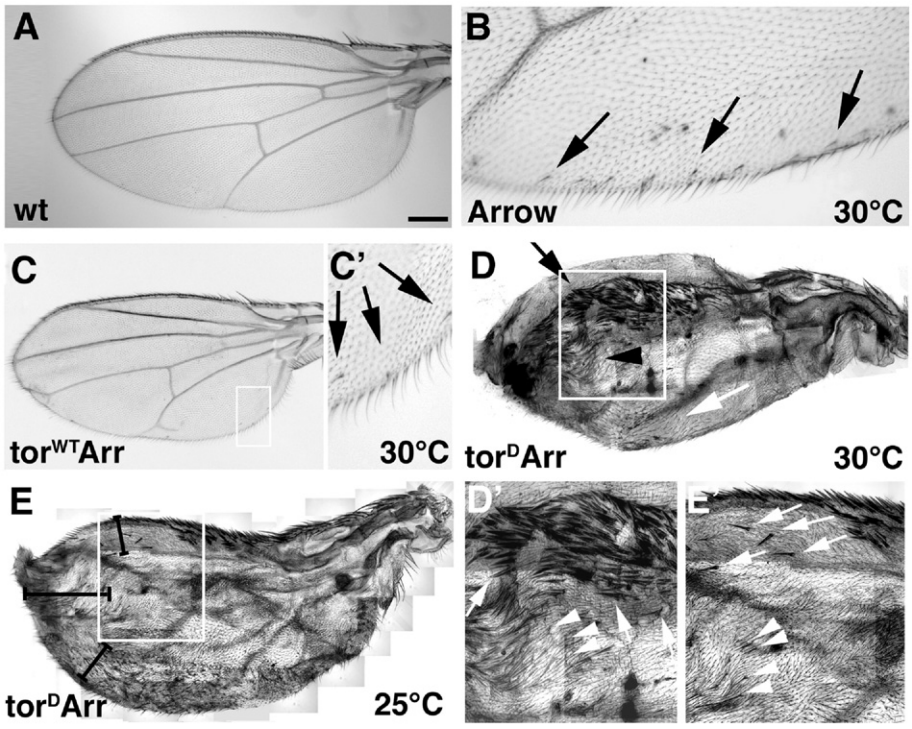

Fig. 5. tor^{D}Arr greatly potentiates Wg signaling. Maximal expression of UAS constructs in the wing was accomplished using the MS1096-Gal4 driver at 30 °C. (A) Wild-type wing, anterior is up. (B) Over-expression of Arrow (UAS-Arrow) induces ectopic margin bristles; ectopic posterior hairs are indicated by black arrows (Wehrli et al., 2000). (C, C′) Few ectopic margin bristles (arrows) are induced by tor^{WT}Arr expression (UAS-tor^{WT}Arr), and minor venation defects occur near the margin. Panel C′ shows magnified view of boxed region in panel C. (D, D′) High level expression of tor^{D}Arr (UAS-tor^{D}Arr) covers most of the wing in bristles and hairs. The bristles and hairs are appropriate for each sector of the wing, which is reflected by the distributions of different types of ectopic bristles: stout triple row bristles are seen near the anterior margin (black arrow), slender double row bristles are seen in the medial–distal sector (arrowhead) and fine hairs are seen posteriorly (white arrow). Because the unequal expression of tor^{D}Arr (driven by MS1096-Gal4) causes distortions in the wing and diminishes wing size, no wing veins are visible in this preparation. In panel D′ some ectopic stout triple row bristles and slender double row bristles are indicated with arrows and arrowheads, respectively. (E, E′) tor^{D}Arr at 25 °C only induces bristles in a band adjacent to the wing margin, demonstrating its dependence on endogenous Wg that originates at the margin (brackets). In panel E′ stout bristles (arrows) and slender bristles (arrowheads) are distinguishable. As in panel D, the wing is distorted due to unequal growth of dorsal and ventral wing blades. To account for these distortions, images for panels D, D′, E, and E′ were collected as bright-field Z-stacks, optically flattened, and assembled as mosaics (see Materials and methods for details). In order to allow for viability of flies shown in Fig. 6B, the wing in panels E and E′ is from a fly containing two copies of tor^{D}Arr but that, like wings in Figs. 6B–F, is heterozygous for the MS1096-Gal4 driver and has half the dose of Wingless (MS1096-Gal4/+; wg^{-}/+; 2× UAS-tor^{D}Arr; see Materials and methods for details). Scale bar=50 μm (A, C); 25 μm (D, E); 12.5 μm (B, C′, D′, E′).

needed to interfere with EGF-receptor signaling and wing vein specification. Thus, as seen in our experiments using embryos, Fz2-Arr can apparently activate Wg signaling independent of ligand in the developing wing. However, the potency of this effect was substantially less than expected for a fully active receptor, which would produce wings covered in margin bristles (described below). This limited activity might simply be due to conformational distortion in the Fz2-Arr fusion protein or might reflect the long-range nature of the Wg signaling gradient in the wing, compared to that of the developing embryo. Evidence for the latter hypothesis is described below.

We reasoned that if Fz2-Arr does generate a ligand-independent but low-level activation of the Wg signaling pathway in the wing, this signal should be amplified by tor^{D}Arr. Indeed, co-expression of the two constructs in wing discs produced wings that were largely covered in margin bristles, except for the more medioproximal region near the wing hinge (Figs. 6B, B′). To test whether the region near the wing hinge is less competent to generate bristles (Ripoll et al., 1988), we induced small *axin*^{S044230} mutant clones to mimic constitutive Wg signaling. Images of 22 wings carrying multiple clones were then projected onto a wild-type wing to map the positions of ectopic bristles. This method produced small clones across all regions of the wing blade, visible as dark spots (not shown), but ectopic bristles were not observed in the central part of the wing near the hinge (Supplementary Fig. 1). A side-by-side comparison of this preparation with the wing in Fig. 5D expressing tor^{D}Arr is shown in Supplementary Fig. 1B; this juxtaposition illustrates that the medioproximal region devoid of bristles is roughly of the same shape and size in both preparations, even though the wing expressing tor^{D}Arr is much smaller. In contrast to the potent synergy seen when tor^{D}Arr +Fz2-Arr was co-expressed (Figs. 6B, B′), tor^{WT}Arr only weakly synergized with Fz2-Arr, resulting in wings with only a few ectopic bristles and minor venation defects (25 °C; Fig. 6D). A similar mild phenotype was observed when full-length Arrow was co-expressed with Fz2-Arr (25 °C; Fig. 6E). Co-expression of Fz2-Arr with Fz2-CFP modestly increased the number of ectopic bristles and caused unequal growth of wing blades, resulted in warping of the wing (25 °C; Fig. 6F),

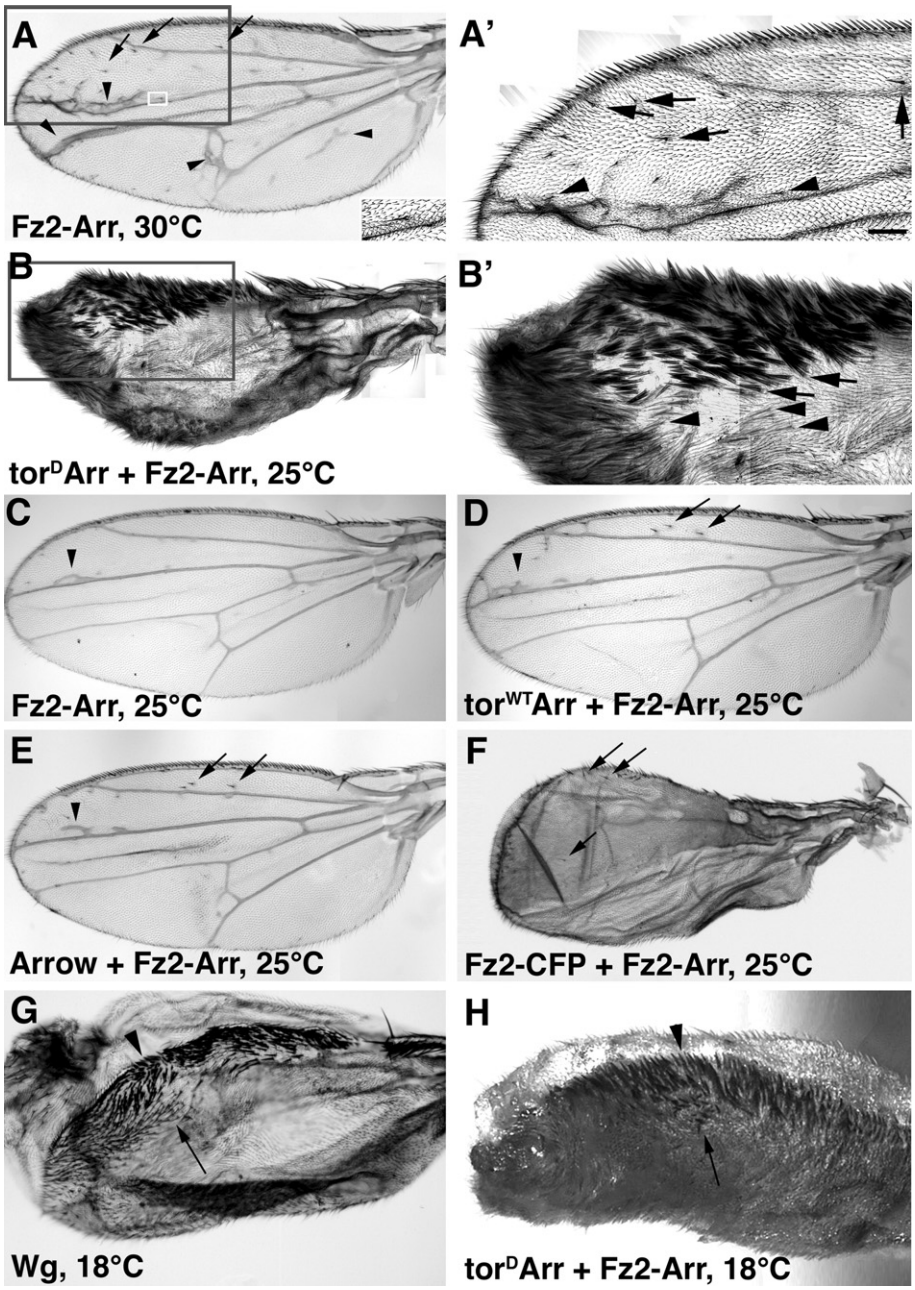

Fig. 6. Synergy between tor^{D}Arr and Fz2-Arr approximates the normal signal transduction levels of Wg ligand. In panel A, A′ expression occurred at 30 °C (as in Fig. 5B–D); while in panels B–F, attenuated Wg signaling at 25 °C permits flies of even the most severe phenotype (e.g., panel B) to survive (see Materials and methods). (A, A′) Bristles induced by Fz2-Arr expression are predominantly near the margin (arrows) but are also found closer to the center of the wing blade (inset); venation defects are apparent (arrowheads), predominantly around vein III–V. In panel A′, ectopic stout triple row bristles and slender double row bristles are indicated with arrows and arrowheads, respectively. Also visible, due to the high contrast, are the much smaller trichomes ('wing hairs') produced by each cell in the wing, as in wild type. (B, B′) The synergistic effects of co-expressing tor^{D}Arr with Fz2-Arr produce wings that are covered in margin bristles. In panel B′ many ectopic stout triple row bristles (arrows) and slender double row bristles (arrowheads) are visible. Trichomes are visible in the area not covered by large bristles, as in wild type. (C) Fz2-Arr alone displays only minor venation defects (arrowhead). (D) Co-expression of tor^{WT}Arr with Fz2-Arr induces minor venation defects (arrowhead) and some ectopic bristles (arrows). (E) Co-expression of Arrow with Fz2-Arr causes minor venation defects (arrowhead) and ectopic bristles (arrow). (F) Co-expression of Fz2-CFP with Fz2-Arr generates ectopic bristles (arrows) and causes loss of wing veins (as in Figs. 5D–E and panels B, B′); unequal growth between dorsal and ventral wing blades distorts the wing. (G, H) Co-expression of tor^{D}Arr and Fz2-Arr re-constitutes normal Arrow function in the Wg signaling pathway. (G) At 18 °C, the levels of Wg ligand over-expression (UAS-Wg) induced by the MS1096-Gal4 driver are sufficiently low to permit flies to complete development. However, this level of Wg expression still induced a band of ectopic margin bristles (arrow); arrowhead indicates the anterior wing margin (the wing is still partly folded). (H) Co-expression of tor^{D}Arr and Fz2-Arr induces a similar number of ectopic rows of bristles as the Wg ligand itself (compare with panel G). In panel G, the wing was mounted; in panel H, the wing was directly photographed to minimize distortions (see Materials and methods). The higher resolution images shown in panels A′ and B′ were generated as described in Fig. 5. Scale bars = 50 μm (A, C–F), (A′, B) 25 μm, (B′) 12.5 μm, (G, H) 32 μm.

whereas expression of Fz2-CFP alone did not cause defects under these conditions (not shown). Taken together, these findings demonstrated that tor^{D}Arr and Fz2-Arr synergize very strongly in the developing wing. Even at 25 °C (which induced suboptimal levels of expression), tor^{D}Arr greatly enhanced the effect of Fz2-Arr alone (compare Fig. 6B with C). As seen in the developing embryo, these results support the conclusion that tor^{D}Arr can amplify even a weak signal initiated by Fz2-Arr.

The potent synergistic effect of expressing Fz2-Arr with tor^{D}Arr raised the question of how their combined signal strength compared to activation of the endogenous receptor by Wg. Because high levels of ectopic Wg expression result in lethality (Noordermeer et al., 1992; Struhl and Basler, 1993), we drove Gal4 expression at 18 °C to obtain flies expressing either exogenous Wg ligand or tor^{D}Arr+Fz2-Arr at similar levels. In both cases, the wings of these flies were markedly distorted, but they expressed similar numbers of ectopic margin bristles (~16 rows), particularly apparent as stout bristles at the anterior wing margin (Figs. 6G, H). Neither of these manipulations produced as widespread an effect as expressing tor^{D}Arr+Fz2-Arr at 25 °C (~25–30 rows of stout bristles and many more slender bristles; Figs. 6B, B′), consistent with the temperature-sensitive nature of Gal4 expression. This result suggests that co-expression of Fz2-Arr and tor^{D}Arr activates the Wg pathway to roughly the same level as expressing exogenous Wg ligand in the same regions. Therefore, the synergistic effect of Fz2-Arr plus tor^{D}Arr approximately reconstitutes the wild-type function of ligand-activated receptors.

tor^{D}Arr function is cell autonomous

The foregoing experiments might be interpreted in three ways: (1) expression of tor^{D}Arr might directly induce Wg transcription or stabilize Wg protein, thereby increasing the level of Wg ligand; (2) tor^{D}Arr might simply propagate the endogenous Wg signal from its source; or (3) tor^{D}Arr might amplify the signal cell autonomously. To distinguish among these possibilities, we investigated the effects of our chimeric receptors in wing imaginal discs of third instar larvae (a stage when the pattern of wing formation is being established). Wg is normally expressed at the dorsoventral compartment boundary of the wing disc and is required for the formation of the entire wing blade (Couso et al., 1994). Therefore, to distinguish among the potential effects of tor^{D}Arr on different aspects of Wg signaling, we expressed tor^{D}Arr in the wing disc and examined them for changes in the expression of either *wg* itself or in *wg* target genes.

One *wg* target gene is *senseless* (*sense*), which is expressed in sensory organ precursor cells (SOP) that will give rise to the margin bristles in the adult wing. As shown in Fig. 7A, Senseless is normally expressed on either side of the stripe of endogenous Wg expression in the wing disc, corresponding to regions of maximal Wg signaling (Nolo et al., 2000). When we expressed tor^{D}Arr throughout the developing wing disc, we observed that the distribution of Senseless expression was greatly expanded (Fig. 7B). This increase in Senseless-positive cells is consistent with the presence of ectopic margin bristles found in the adult (compare with Fig. 5D). Since cells in these regions behaved as if they had been exposed to maximal levels of Wg, we also asked whether the *wg* gene itself was induced in response to tor^{D}Arr expression, using a Wg-lacZ enhancer trap construct as a reporter for Wg expression in these preparations. As shown in Figs. 7A–B, the levels of *wg* gene expression were unchanged by the expression of tor^{D}Arr throughout the wing disc, indicating that the effect of this construct on Senseless expression was not simply due to the induction of ectopic Wg expression. As a complementary method, we also examined the distribution of Wg using an immunostaining protocol that visualizes extracellular Wg (after Strigini and Cohen, 2000). As shown in Figs. 7C′ and D′, we found no detectable differences in the levels of secreted Wg in these preparations compared to controls.

A second possible explanation for the effects of tor^{D}Arr is that it augments the propagation of the endogenous Wg signal in a continuous fashion from cell to cell. This type of propagation would be predicted to require an unbroken chain of Senseless-positive cells originating from the stripe of Wg expression at the dorsoventral compartment boundary, while isolated patches of cells expressing tor^{D}Arr would not be expected to express Senseless. To test this possibility, we used the MARCM technique (Lee and Luo, 2001) to induce GFP-labeled clones of cells expressing tor^{D}Arr in wing discs, and then immunostained the preparations to detect Senseless expression. As shown in Fig. 7E, clones that were physically separated from the stripe of Wg expression (and the adjacent rows of cells expressing endogenous Senseless) nevertheless expressed Senseless, indicating high levels of Wg signal transduction in these regions (yellow arrows, in Fig. 7E). These results show that the effect of tor^{D}Arr on Senseless expression is not simply due to enhanced propagation of the Wg signal from cell to cell; rather, these results indicate that tor^{D}Arr function is cell autonomous.

In adult wings, unmarked clones of tor^{D}Arr-expressing cells formed ‘islands’ of margin bristles that corresponded to the wing sector in which they were expressed. For example, Fig. 7F shows an example of an island of stout bristles (arrowhead) in the anterior portion of the wing of the type normally found in the triple row of bristles in the anterior wing margin. In contrast, tor^{D}Arr clones in more posterior regions expressed slender hairs (arrows), corresponding to hairs normally seen in posterior region of the wing. The occurrence of such tufts of bristles that are physically separated from the wing margin provides further evidence that tor^{D}Arr does not simply augment the propagation of an endogenous Wg signal through adjacent cells.

Because Senseless expression depends on the highest levels of Wg signaling, it provides an ‘all-or-nothing’ readout for this signal transduction pathway. Therefore, we also examined another *wg* target gene, *Distal-less* (*Dll*), which responds to Wg signaling in a more graded fashion and therefore might reveal more subtle changes in signaling levels within clones expressing tor^{D}Arr. Dll is endogenously expressed throughout the wing pouch: its highest levels occur at the dorsoventral compartment boundary (coinciding with the stripe of Wg expression), while gradually declining levels across the rest of the wing pouch correspond to the distance of cells from the Wg

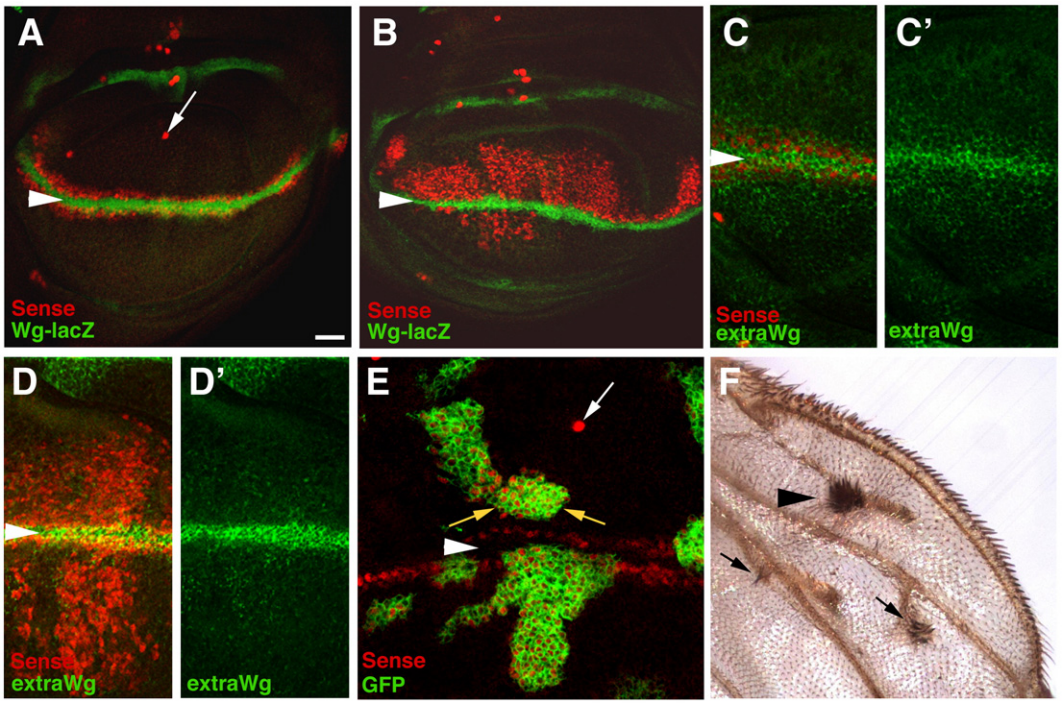

Fig. 7. tor^{D}Arr functions cell autonomously. In all confocal micrographs, dorsal is up, and white arrowheads mark the D/V boundary. Larvae were reared at 30 °C to induce maximal tor^{D}Arr expression levels. (A) Wg enhancer trap expression (Wg-lacZ, green) along the dorsoventral (D/V) compartment boundary (the future wing margin, white arrowhead) is straddled by expression of the *wg* target gene *senseless* (*sense*, red) in sensory organ precursor cells (SOP). (B) Expression of tor^{D}Arr in the wing pouch with MS1096-Gal4 induces many additional Senseless-positive cells (red), correlating with future bristle cells. Wg-lacZ expression is unchanged by tor^{D}Arr expression. (C) Extracellular Wg is visualized using a protocol that allows immunostaining of secreted Wg (C′ green; as in Strigini and Cohen, 2000), demonstrating the spread of Wg ligand away from the source at the D/V boundary, which is flanked by Senseless expressing cells (red; compare to panel A). (D) Expression of tor^{D}Arr induces many ectopic Senseless expressing cells (red), suggesting maximal transduction of the Wg signal, yet no increase in extracellular Wg is apparent. Panel D′ shows the Wg channel alone. (E) Both the endogenous expression pattern of Senseless and the ectopic Senseless cells are visible in the same tissue, but all ectopic Senseless-positive cells are confined to clones expressing tor^{D}Arr (GFP-positive, green). Note that clones need not be directly adjacent to Wg-expressing cells to be capable of inducing Senseless expression (yellow arrows). The endogenous pattern of Senseless expression can be seen flanking the D/V boundary (arrowhead) is apparent, plus a large Senseless-positive cell resides in the center of the presumptive wing blade (arrow, compare to wild type, in panel A). (F) The expression of tor^{D}Arr in clones is manifested as tufts of bristles in the adult wing. Several clones are shown containing either stout bristles of the anterior triple row type (arrowhead) or slender bristles of double row type (arrows). Note that these clones form 'islands' that are not connected to the wing margin, which is the endogenous source of Wg (as noted above). Scale bars = 50 μm (A, B), 25 μm (C, D), 10 μm (E), 8 μm (F).

source (Diaz-Benjumea and Cohen, 1995; Neumann and Cohen, 1997; Zecca et al., 1996; Campbell and Tomlinson, 1998). When tor^{D}Arr was expressed in a clone non-adjacent to the Wg source at the wing disc margin, Dll expression was also markedly increased in this region (Figs. 8A, B, arrows). In particular, the highest levels of Dll within tor^{D}Arr-expressing clones were detected on the side nearest the dorsoventral boundary (D/V) where endogenous Wg is expressed (indicated by arrowheads).

To account for potential artifacts that might stem from irregularities in nuclear position or tissue morphology within these preparations, we acquired serial stacks of optical sections, selected a region of interest (white box, Fig. 8A) and quantified the pixel intensity (see Materials and methods). The total intensity of fluorescence of the projection was measured and plotted against the distance from the D/V boundary. As shown in Fig. 8C, this method demonstrated that the graded distribution of Dll expression within a clone was similar to the distribution of endogenous Dll with respect to the D/V boundary, while the highest Dll protein levels within the clone were comparable to the level of Dll at the Wg stripe. Examining the levels of Dll expression in a number of clones of this type in different preparations yielded similar results (not shown; see also Figs. 8D–G).

This pattern of Dll expression might simply arise in direct response to the endogenous Wg gradient, whereby cells closest to the Wg source express the most Dll. By this model, clones at greater distances from the Wg source would display overall reduced Dll expression levels. Alternatively, an interface with organizer properties in the developing wing might be generated at the boundary of tor^{D}Arr-expressing clones (similar to the dorsoventral boundary itself), which in turn might control the relative levels of Dll within the clone. By this scenario, maximal Dll levels would be similar within any clone, regardless of its position in the disc. Our examination of multiple clones supported the first possibility, but the folded nature of the wing pouch in regions distant from the D/V boundary complicated this analysis (not shown). Therefore we lowered the levels of tor^{D}Arr expression by rearing the animals at 25 °C, allowing us to examine clones in the less folded regions of the wing pouch. As illustrated in Figs. 8D and E, clones that were closer to the source of Wg (arrowhead) displayed comparatively high levels

of Dll expression, while more distant clones expressed lower levels (yellow arrow). In addition, Dll levels within the tor^{D}Arr clones were clearly higher than in the surrounding tissue, with Dll expression in both clonal and non-clonal regions declining as a function of distance from the Wg source. These trends were also apparent in Z-stack projection images of these preparations: Figs. 8F–G show a lower magnification of the same preparation in panels D–E; despite the higher levels of total fluorescence that result from this method, enhanced levels of Dll expression could clearly be distinguished within clonal regions closer to the endogenous source of Wg at the D/V boundary (arrowhead). The most parsimonious explanation for these observations is that the cell-autonomous action of tor^{D}Arr is to amplify Wg signaling induced by endogenous Wg ligand, rather than the alternative model that tor^{D}Arr induces a maximal response, regardless of the level of Wg present. These results further support our conclusion that Arrow participates in two distinct aspects of Wg signal transduction, as discussed below.

Our analysis of Fz2-Arr and tor^{D}Arr function in the embryo demonstrated that these two constructs can synergize and, in the absence of Wg ligand, tor^{D}Arr can use the signal generated by Fz2-Arr in order to increase the overall signal. Since synergy between Fz2-Arr and tor^{D}Arr is also readily apparent in the wing (Fig. 6B), we asked whether loss of the endogenous Wg ligand in clones within the developing wing disc could be overcome by co-expression of Fz2-Arr and tor^{D}Arr in those cells. For clarity, we used the high-threshold target Senseless as a marker. Clones of wg^{-} cells were induced in first instar larvae to create clones that would cross the dorsoventral compartment boundary, thereby disrupting Wg expression on both sides of the boundary. The wg^{-} clones were also positively marked with GFP using the MARCM technique. As shown in Fig. 9, cells inside the wg^{-} clones failed to express Senseless (Fig. 9B, arrow), except for cells immediately adjacent to Wg-expressing cells, which received sufficient Wg by diffusion from the surrounding wild-type cells to induce Senseless expression (Fig. 9C). These results verify that the non-autonomous activation of Senseless by Wg extends over only one cell diameter. In order to address whether the synergistic effects of Fz2-Arr+tor^{D}Arr were truly independent of Wg, we expressed these two constructs, along with GFP, in wg^{-} clones. The largest clone obtained by this method slightly distorted the wing and was ~10 cell diameters across at the dorsoventral boundary (Figs. 9D–F). Within this region, all wg^{-} cells expressed the high-threshold target Senseless (region between arrowheads in Fig. 9F). This result is consistent with our model that Fz2-Arr+tor^{D}Arr induces ligand-independent activation of signaling in the developing wing, as observed in the embryo (Figs. 4D, E).

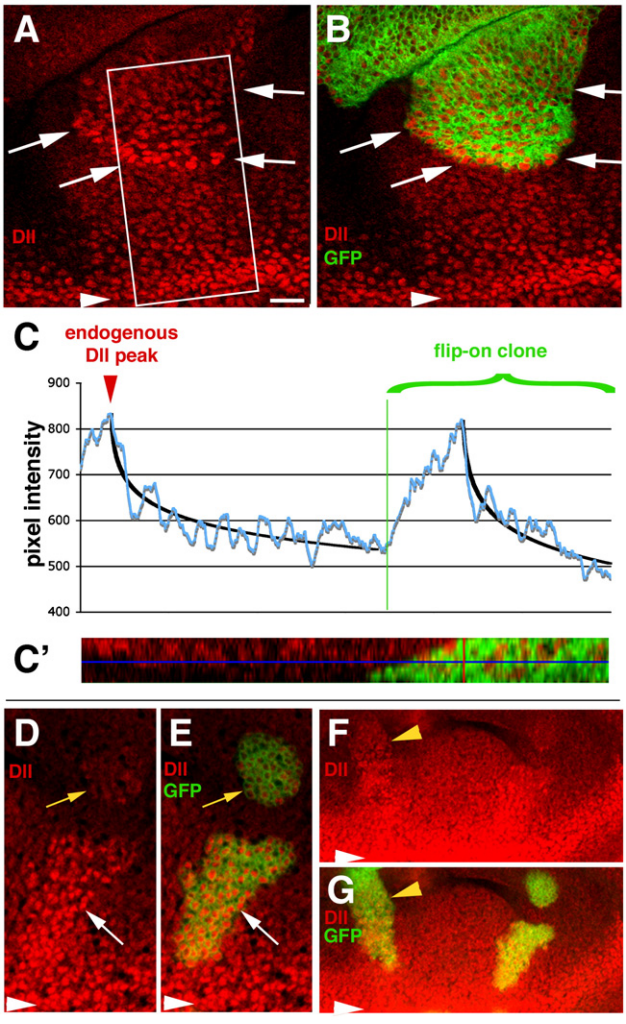

Fig. 8. tor^{D}Arr amplifies the Wg signal in response to available ligand. For panels A–C, larvae were reared at 30 °C, while for panels D–G, larvae were reared at 25 °C to maintain lower tor^{D}Arr expression levels. (A, B) tor^{D}Arr-expressing clones (green) also exhibit a cell-autonomous increase in the expression of the *wg* target gene *Distal-less* (*Dll*, red). Within the clone, Dll expression diminishes in a graded fashion away from the source of Wg at the D/V boundary (indicated by arrows), reflecting the Wg dependence of signal potentiation by tor^{D}Arr. (C) The endogenous Dll gradient profile matches the Dll gradient generated in a clone expressing tor^{D}Arr. In order to accommodate the three-dimensional nature of this tissue, Dll staining in the region indicated in panel A was determined and the graph indicates expression levels as a function of the distance from the endogenous signal peak (at the D/V boundary, arrowhead in A; see Materials and methods). As apparent in panel A, a sharply defined edge of high-level expression is visible at the border of the clone facing the D/V boundary. The gradual increase of Dll expression levels reflects averaging across the curved boundary of the clone and the slanted angle of the epithelium. The shape of the gradient fits a logarithmic curve. (C′) A vertical section reveals that tissue folds position the GFP expressing clone at an angle similar to the Dll profile observed in panel C and explains why the Dll increase appears gradual. This vertical section through the Z-stack along the middle of the box shown in panel A; green, GFP; red, Dll; the blue horizontal line marks the level of the section shown in panels A and B. (D, E) A tor^{D}Arr-expressing clone (green, white arrow) near the D/V boundary (arrowhead; the source of Wg) expresses higher levels of Dll than a more distant clone (yellow arrow), illustrating that the level of signal amplification by tor^{D}Arr is proportional to the level of Wg. (F, G) Lower magnification of a Z-stack projection of the preparation containing the clones shown in panels D and E. An additional elongated clone (yellow arrowhead) shows a graded decline with distance from the Wg source, though adjacent tissue expresses considerably lower levels of Dll. Scale bars=17 μm (A, B), 10 μm (D, E), 20 μm (F, G).

Discussion

Our data best fit a model in which Arrow functions in two distinct steps in the Wg signaling pathway (Fig. 10). First,

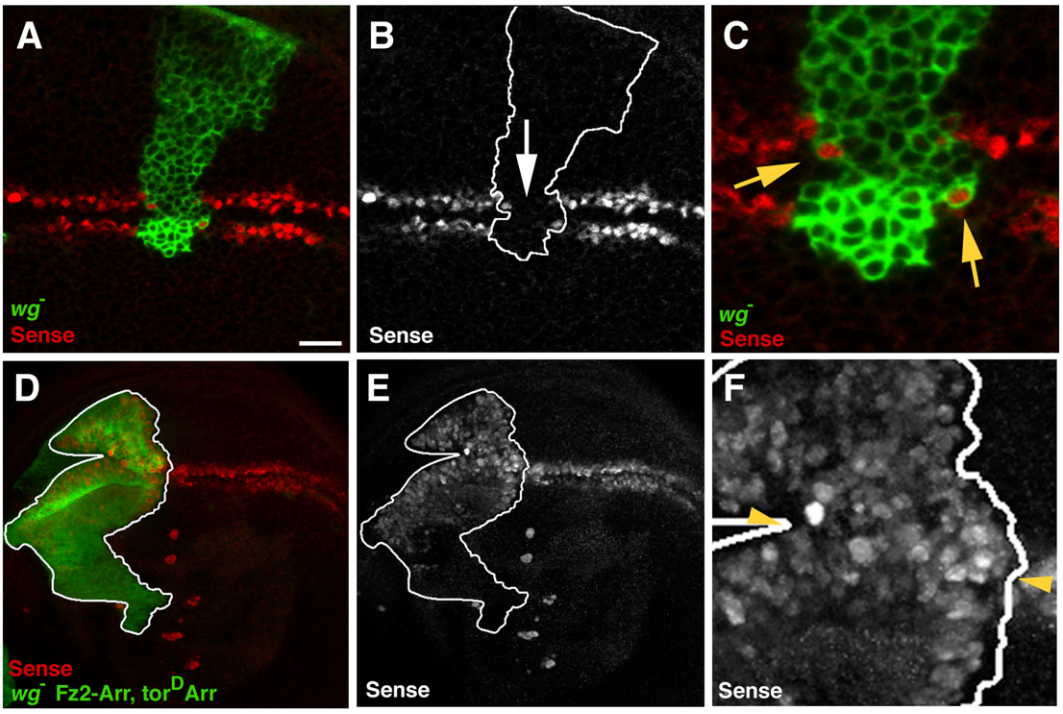

Fig. 9. Induction of Senseless expression by Fz2-Arr+torDArr in wg^- clones. (A–C) A wg^- clone (green) intersects the endogenous Senseless (red) stripe flanking the endogenous Wg expressing cells at the D/V boundary. Wg from surrounding wild-type tissue can diffuse and rescue adjacent Senseless expression in wg^- cells (yellow arrows in panel C), while the remainder of the clone fails to express Senseless (white arrow in panel B). Panel B shows a schematic projection of the clone boundary in panel A. Panel C shows a higher magnification of panel A. (D–F) wg^- clone (green) expressing Fz2-Arr+tor^DArr induces Senseless expression across the entire clone (region between yellow arrowheads in panel F), extending well beyond the single row of cells at the clone boundary seen in panel C. The clone distorts the wing disc and has its narrowest point at the D/V boundary (between arrowheads); panels D–F show a projection of a partial Z-stack to accommodate this distortion. Scale bars = 10 μm (A, B), 4 μm (C), 30 μm (D, E), 4.2 μm (F).

Arrow is required for the initiation of Wg signaling, when it functions as a requisite subunit of the Wg receptor. Subsequently, Arrow is also required in a second *downstream* step that serves to amplify signals initially generated by the receptor complex. Using chimeric receptor constructs, we have shown that these two steps can be functionally separated: Fz2-Arr was able to initiate a signal in the absence of ligand but could only weakly amplify the resultant signal (Figs. 1A–C). In contrast, tor^DArr quite potently amplified Wg signaling (Figs. 2B, 5D–7, 7, 8) but could not initiate a signal on its own (Fig. 1M, Fig. 3), thus distinguishing the initiation step from the amplification step. Importantly, our data also showed that wild-type Arrow can normally amplify endogenous Wg signals, as revealed in embryos expressing Fz2-Arr (Figs. 1B, D). In contrast, net Wg signaling in the absence of Arrow (*arrow*$^-$ mutants) was significantly weaker than in the presence of Arrow (Fig. 1C). Consistent with this finding, over-expression of Arrow in the developing wing was capable of potentiating endogenous Wg signaling (Fig. 5B). Lastly, we showed that the two steps distinguished by Fz2-Arr and tor^DArr could be largely reconstituted by co-expressing the two constructs, a genetic manipulation that almost completely restored the normal level of ligand-stimulated Wg signaling that occurs in the presence of wild-type Arrow and Fz2 (Figs. 4D–E, 9D–F).

Our model leaves open the possibility that Arrow-mediated amplification might simply increase the signaling activity of the receptor. However, the more likely mechanism for signal potentiation by Arrow is the downstream inactivation and degradation of Axin, since Axin binds to Arrow/LRP (Mao et al., 2001; Tolwinski et al., 2003). Consistent with our model (Fig. 10), Axin is primarily localized to the cytoplasm but translocates to the membrane in the presence of Wg/Wnt, a process that is Dishevelled-dependent (Cliffe et al., 2003). The mechanisms regulating Dishevelled activation remain controversial but may require Dishevelled–Frizzled interactions at the time of receptor activation (Wong et al., 2003), followed by interactions between Dishevelled and Axin (Julius et al., 2000). This sequence may then result in destabilization and partial inhibition of the Axin complex at a level that is sufficient to induce signaling without amplification. Indeed, over-expressed Dishevelled can induce Wg signaling in the complete absence of Arrow, a process that is Wg-independent (Wehrli et al., 2000). However, to generate a strong signal under physiological conditions, activation of Dishevelled likely results in a conformational change in Axin, which in turn promotes the interaction of Axin with Arrow/LRP. In support of this model, work in fibroblast cells has shown that Axin–LRP5 interactions occur only after initiation of the Wnt signaling cascade at the membrane (Mao et al., 2001). This Axin–LRP interaction relies on sequential phosphorylation of conserved PP(S/T)P sequences within Arr/LRP by GSK-3β kinase, followed by phosphorylation by CK1γ (Davidson et al., 2005; Zeng et al., 2005), but whether these modifications are also controlled by Wnt signaling remains controversial. Work from Tamai et al.

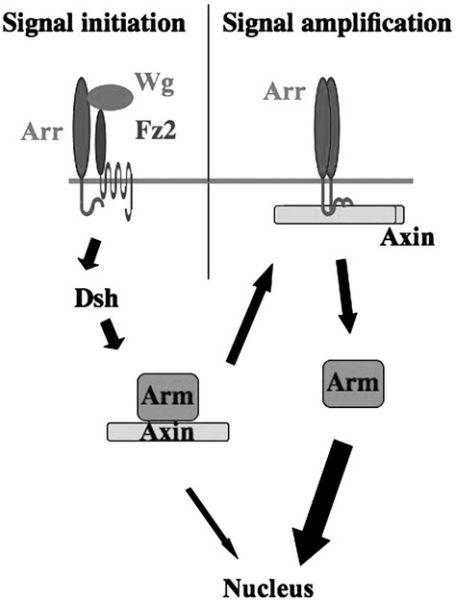

Fig. 10. A two-step model for Wg signal transduction. The Wg receptor complex consisting of Arrow and Frizzleds initiates the cytoplasmic cascade in response to Wg binding. Dishevelled transmits this response to the Axin complex and may destabilize the complex sufficiently to transduce a minor signal to the nucleus, via free Armadillo. For maximal signaling, Axin relocates to the cell membrane, where it interacts with clustered Arrow/LRP and becomes inactivated. Armadillo may then be released from Axin and newly synthesized Armadillo is no longer destroyed, resulting in amplified transcriptional activation in the nucleus.

(2000) also provides support for our two-step model. Over-expression of LRP6 in *Xenopus* embryos appears to potentiate Wnt signaling rather than trigger a new signal, since co-injecting the Wnt inhibitor sFRP completely blocked this potentiating effect. Currently, the best candidate Wnt that provides this signal endogenously is maternal Wnt11, which is also required for dorsal axis formation (Tao et al., 2005). Taken together, these findings suggest that Axin is not likely to interact with Arr/LRP during the *initial* activation of the receptor, but rather, Arr/LRP–Axin interactions occur later, consistent with the proposed amplification function of Arr/LRP.

Notable differences between our data and those of others are that we find a strict dependence of tor^{D}Arr activity on the presence of Wg ligand, Frizzleds and Dishevelled. While other reports have suggested that over-expressed LRP or extracellularly truncated LRP may have signaling activity independent of Wg/Wnt ligands, Frizzleds, or Dishevelled (Brennan et al., 2004, Li et al., 2002, Cong et al., 2004, Mao et al., 2001), we found that the activity of tor^{D}Arr activity clearly required these components. Since we used either null mutations or strong hypomorphic alleles of Wg pathway components for our analysis, it is possible that the endogenous signaling levels in our experiments fell below the threshold required for smooth cuticle specification. Conversely, it is possible that the apparent ligand independence of LRP signaling in previous reports was due to residual levels of Wnts, either derived from autocrine secretion or due to the presence of Wnts in the serum used in these studies. Wnts have now been detected in adult human serum (Wnt-11, States et al., 2006; Wnt-9a, Barnea et al., 2005) and are likely to be present in greater abundance in fetal serum used in tissue culture. In addition, previous observations suggesting that LRPs can activate the Wnt/Wg signaling pathway independent of Frizzled or Dishevelled may also have been compromised by incomplete knockdowns of these genes, or they may have been complicated by non-specific effects stemming from the high levels of expression achieved in the transient transfection experiments used in these studies. Our findings may therefore provide an alternative interpretation for this body of work: namely, that Arr/LRP may not activate signaling pathways other than Wnt but instead functions in the Wnt pathway at two distinct steps.

The most conclusive proof that Arrow plays sequential roles in Wg signal initiation and signal amplification would ideally link the in vivo function of these two steps directly to specific protein–protein interactions that are known to occur during development. Since biochemical interactions obtained from over-expression studies in vitro may not accurately reflect authentic functions in developing animals, we engineered two molecularly defined fusion proteins, Fz2-Arr and tor^{D}Arr, whose signaling activity could be directly assayed in vivo. The differences in activity of these constructs (which discriminate between ligand-independent and ligand-dependent signaling) revealed differences in function that are best explained by our model that the two chimeric proteins act during distinct steps in signal transduction. This finding is also consistent with available biochemical data from in vitro studies, as discussed above. A direct link between distinct signal transduction steps and cell biological events might also be obtained by selectively disrupting and re-activating the signaling mechanism. For example, it might be possible to design temperature-sensitive versions of different components of the Wg signaling pathway to examine how regulated changes in Wg signaling affect Axin localization or Armadillo accumulation. We are currently generating mutations of this type to selectively disrupt the Wg signaling pathway between the initiation and amplification steps indicated by our model.

Tissue-specific differences in Wnt signaling and the role of signal amplification

By using transgenic animals for an in vivo analysis of Arrow function, we were able to decipher tissue-specific differences in the activity of our Fz2-Arr and tor^{D}Arr constructs that might otherwise have escaped detection. Comparing the relative potencies of our constructs in embryos versus developing adult wings revealed interesting trends that were context-specific. In *wg*$^{-}$ mutant embryos (Fig. 4) the relative activities of our constructs were 1× Fz2-Arr ≪ Fz2-Arr + tor^{D}Arr < 2× Fz2-Arr (Figs. 1–4). Thus, higher levels of Fz2-Arr alone proved to be more potent in the embryo than a combination of Fz2-Arr and tor^{D}Arr. In contrast, their relative activities in the developing wild-type wing were 2× Fz2-Arr ≪ 2× tor^{D}Arr ≪ Fz2-Arr + tor^{D}Arr (Figs. 5E, 6B and C). Thus, while tor^{D}Arr alone was more potent than Fz2-Arr alone, the combined expression of the two constructs provided by far the most potent activity (Fig. 5E,

6B), revealing that the two constructs must serve distinct functions that act synergistically in this tissue.

A likely explanation for this result is that Fz2-Arr contributes a specific function to the Wg signaling mechanism that is otherwise lacking, presumably by acting as an activated receptor. This finding also underscores the dependence of tor^{D}Arr on the prior activation of a Wg signal, which it then potentiates. That this potentiation event appears much stronger in the wing than in the embryo suggests an intriguing difference in the mechanisms of Wg signal transduction within these two developmental contexts. In the wing, where long-range Wg gradients need to be appropriately interpreted, our data suggest the presence of an endogenous amplification mechanism that can be exploited by elevated levels of Arrow or by tor^{D}Arr. By contrast, this type of amplification may be reduced or missing in the embryo, where tor^{D}Arr was markedly less potent. Whereas the width of the embryonic segment requiring Wg function to form smooth cuticle is ~6 cells, the range of the Wg gradient in the wing is at least an order of magnitude larger. Hence, variations in the mechanism controlling the spread of Wnt/Wg ligands and subtle differences in their signal transduction pathways in different contexts would explain the adaptations that allow different tissues to respond to short- versus long-range signaling by these morphogens.

A long-standing question in developmental biology has been on how cells faithfully detect and respond to very low morphogen concentrations. Our identification of a mechanism that allows cells to amplify the Wg signal may provide new insight into this important problem. The detection of Wg signals in developing tissues may be affected by many factors but will critically depend on the concentrations of the individual constituents of a Frizzled-Arrow-Wg complex. While the endogenous distribution of active Wg remains somewhat uncertain in any system, it has been shown that Fz2 and Arrow are inversely regulated by Wg signaling (Cadigan et al., 1998; Marois et al., 2006; Rives et al., 2006). Cadigan et al. (1998) proposed that such control of Fz2 expression might shape the Wg gradient, so that receptor concentrations would be higher in regions where Wg levels were lower, thereby driving the assembly of the receptor–ligand complex. In the context of our model, over-expression of Arrow would therefore be expected to increase signaling both by increasing available receptor levels and by potentiating signaling by the inactivation of Axin (a negative regulator of Wg signaling). A similar type of mechanism might also exist in other signaling pathways, providing a means of enhancing a signal through a positive feedback loop or antagonizing downstream inhibitors of the pathway. Signal amplification of the type that we have shown for the Wg pathway may therefore be a general principle used to potentiate the signal in shallow parts of other long-range morphogen gradients.

Materials and methods

Embryonic cuticle assay

UAS constructs were expressed with either ptc-Gal4 or prd-Gal4 drivers, as previously described (Wehrli et al., 2000; Tolwinski et al., 2003). Fz2-Arr was expressed in *fz*$^{-}$ *fz2*$^{-}$ mutants in the genotype hs-flipase; prd-Gal4/UAS > Fz2-Arr; *fz*^{H51} *fz2*^{C1} germ line clones (glc)/*fz*^{H51} *fz2*^{C1} (Figs. 1D, L), using a prd-Gal4 insertion on the 2nd chromosome (gift of Naz Erdeniz). Expression of UAS > Fz2-Arr and UAS > tor$^{WT/D}$Arr was achieved in the genotype wg^{CX4}/wg^{CX4}; prd-Gal4/UAS > Z ('Z' denotes the construct expressed). Fz2-Arr was expressed in one or two copies from the 3rd chromosome in embryos of the genotype hs-flipase; FRT42B *arr*^{2} glc/Df(2)8–104; prd-Gal4/[1× or 2×] UAS > Fz2-Arr (Df(2)8–104 deletes *arrow*; Figs. 1D, I). Reduced Arrow expression was achieved in embryos of hs-flipase; FRT42B *arr*^{2} glc/Df(2)8–104 UAS > Arr; prd-Gal4/+ (Fig. 1J); reduced expression of Fz2 was achieved in hs-flipase; prd-Gal4/UAS > Fz2myc; *fz*^{H51} *fz2*^{C1} FRT2A germ line clones (glc)/*fz*^{H51} *fz2*^{C1} (Fig. 1K).

Embryos were scored as fully rescued in prd-Gal4 experiments if four abdominal bands of smooth cuticle cleanly separated interposed denticle bands. Synergistic interactions with our Fz2-Arr construct were determined by measuring the extent of full rescue at 25 °C, in the genotype wg^{CX4} UAS > Z/wg^{CX4}; UAS > Fz2-Arr/prd-Gal4 ('Z' denotes the construct expressed). Values were compared by Fisher's Exact Test with two-tailed *P* values, using Prism 3.0 software (GraphPad Software Inc.). Results were considered significant if $P < 0.05$.

Wings

MS1096-Gal4 was used to drive expression of our UAS constructs in the developing wing, and expression was modulated by rearing flies at the different temperatures, as noted (Wehrli et al., 2000; Tolwinski et al., 2003). Despite the low levels of Gal4 activity expected at 18 °C, flies that co-expressed tor^{D}Arr and Fz2-Arr under the control of MS1096-Gal4 exhibited poorly viability, even at this temperature. To suppress this lethality, we used *wg*$^{-}$/+ flies to attenuate Wg signaling and took advantage of the diminished Gal4 expression in heterozygous females, allowing us to test these constructs at 25 °C. We then assayed females of the genotype +/MS1096-Gal4; wg^{CX4} UAS>Z/+; UAS > Fz2-Arr/+ ('+' denotes wild type). For consistency, we used the same wg^{CX4} UAS > Z recombinant chromosomes that we used to test for synergy by assaying cuticle phenotypes (Fig. 4). 'Z' constructs are Fz2-Arr, Arrow, Fz2-eCFP, Wg (Wehrli et al., 2000; Tolwinski et al., 2003), tor^{WT}Arr and tor^{D}Arr (this study). In order to distinguish synergy from simple additive effects, we compared the effect of two copies tor^{D}Arr (Figs. 5E, E′) and two copies of Fz2-Arr (Fig. 6C) to the combined effect of one copy of Fz2-Arr plus one copy of the constructs shown in Figs. 6B–F. Torso wild-type (tor^{WT}) or torso dominant (tor^{D}, torso^{4021} Y327C, Sprenger and Nüsslein-Volhard, 1992) extracellular domains (torso V398) were fused with a 7-amino-acid linker to Arrow (A1451) at the extracellular face of the transmembrane domain, generating tor^{WT}Arr and tor^{D}Arr, respectively. Fusion constructs were generated by a combination of PCR, restriction cloning and yeast recombination (Tolwinski et al., 2003); details are available on request.

The MARCM technique (Lee and Luo, 2001) was used to induce GFP-marked clones expressing tor^{D}Arr in the genotype heat shock > flipase MS1096-Gal4; tubulin > Gal80 FRT40A/ck^{13} y^{+} FRT40A; UAS > CD8-GFP/UAS > tor^{D}Arr. 2nd instar larvae were heat shocked for 1 h at 38.5 °C, then reared at 30 °C (or 25 °C for Figs. 8D–G) and dissected as climbing 3rd instar larvae. CyO wg^{lacZ} is a Wg enhancer trap (wg^{en11}, Schmidt-Ott and Technau, 1992) inserted on the CyO balancer chromosome.

Immunohistochemistry

Discs were dissected and stained as previously described (Wehrli et al., 2000). Primary antibodies used in this study were mouse anti-Dll (1:500, gift of Ian Duncan; Duncan et al., 1998; Vachon et al., 1992), guinea pig anti-Senseless (1:1000; gift of Hugo Bellen); chicken anti-GFP (1:1000, Aves laboratories; Tigard, OR; gift of Gary Ciment), rabbit anti-lacZ (1:2000, Abcam), rabbit anti-Arrow (1:15000; gift of Steve DiNardo; Rives et al., 2006). Secondary antibodies used were Alexa488 and Alexa546 (Molecular Probes, Eugene, OR). Images were collected using a Zeiss Axiovert LSM5 Pascal laser-scanning microscope. To quantify Dll expression, Z-stacks were imported into ImageJ, and pixel counts of the regions of interest were exported to Excel for subsequent analysis.

Quantification of expression levels in situ

(a) To quantify prd-Gal4-driven lacZ expression and Fz2-Arr expression, embryos from the cross prd-Gal4×UAS>lacZ were raised at 28 °C, then fixed, and labeled with rabbit anti-lacZ (Abcam) followed by an Alexa488 secondary antibody. The preparations were then imaged by confocal microscopy, using settings that were adjusted to prevent saturation. Z-stack projections of the images were then imported into ImageJ. The average fluorescence for each stripe was determined in multiple embryos of each genotype examined and exported into Excel for analysis.

(b) To analyze Fz2-Arr in wg^{null} or arr^{null} mutants, embryos were collected at 30 °C, then double immunostained with rabbit–anti-myc (Santa Cruz) plus Alexa488 and mouse–anti-lacZ 40a (Developmental Studies Hybridoma Bank) plus Alexa546. LacZ staining was used to identify heterozygous embryos carrying the CyO, eve-lacZ chromosome (gift of Sarah Smolik), which were then excluded from the analysis. Images were collected and processed as described above. Unstained embryos were used to determine background levels, which were subtracted to yield the fluorescence levels given in the text.

(c) To analyze the effects of our constructs in wing discs, male larvae expressing UAS constructs of Arr, tor^{WT}Arr, and tor^{D}Arr under the control of the MS1096-Gal4 driver were reared at 30 °C; GFP was also ubiquitously expressed in these animals to provide an internal reference (ubiquitin > GFP, Datar et al., 2000). Construct expression was visualized by staining for the cytoplasmic domain of Arrow (anti-Arr primary antibody, followed by Alexa546 secondary antibody) and compared to GFP fluorescence. The ratio of [Alexa 546 florescence]/[GFP fluorescence] was determined for the wing pouch (as described above for Dll). For endogenous Arrow, expression levels were found to be minimal at the D/V boundary and maximal at the dorsal and ventral edges of the wing pouch (Supplementary Figs. 2A–D; see also Rives et al., 2006; Marois et al., 2006); Arrow-associated immunofluorescence in these preparations therefore represented the combination of our Arrow constructs plus endogenous Arrow levels (see also Supplemental Figs. 2A–D). The maximal and minimal ratios obtained by this assay were: for UAS-Arr, 3.05±0.72 and 1.4±0.48, respectively; for UAS-tor^{WT}Arr, 2.24±0.53 and 1.09±0.4, respectively; for UAS-tor^{D}Arr, 2.71±0.59 and 1.18±0.28, respectively (Supplementary Fig. 2D). Expression levels for these three constructs were not significantly different.

Photography

Cuticles and mounted wings were photographed on an Axioplan2 microscope with an AxioCam MRm Zeiss digital camera. For Figs. 5D, E and 6A, B, Z-stacks of mounted wings were collected using a 40× objective, optimally flattened using the Image Pro Plus software and assembled as mosaics in Photoshop. Alternatively, Z-stacks of wings from living flies were collected directly using a Leica MZFL-III stereomicroscope and photographed with an Optronics Magna Fire CCD Camera; Z-stack projections of the preparations were then generated using an Image Pro Plus workstation. Photomontages were assembled using Adobe Photoshop 7.0.

Acknowledgments

We are grateful to Drs. Gary Ciment, Hugo Bellen, Ian Duncan, Barry Dickson, Naz Erdeniz, Sarah Smolik, Philip Copenhaver, Tracy Swanson and Steve DiNardo for providing critical reagents for this work. We also acknowledge the Bloomington Stock Center and the Developmental Studies Hybridoma Bank (DSHB) for providing us with fly stocks and antibodies, respectively. We thank Drs. Jan Christian, Philip Copenhaver, Steve DiNardo, Naz Erdeniz, Brian Johnstone, Richard Maurer and Mike Forte for comments on the manuscript and Rachel Dresbeck for editing the manuscript. We would also like to thank Drs. Stephanie Kaech Petri, Bruce Schnapp and John Williams for helping with fluorescence imaging. Jocelyn Early provided excellent technical assistance. This work was started in the laboratory of Steve DiNardo and initially supported by grant GM045747; the confocal microscope used in this study is part of the Metal Ion Core Facility, supported by P01-GM067166. This work was supported by NIH grant GM67029 to M.W.

Appendix A. Supplementary data

Supplementary data associated with this article can be found, in the online version, at doi:10.1016/j.ydbio.2007.03.005.

References

Axelrod, J.D., Matsuno, K., Artavanis-Tsakonas, S., Perrimon, N., 1996. Interaction between Wingless and Notch signaling pathways mediated by Dishevelled. Science 271, 1826–1832.

Babu, P., 1977. Early developmental subdivisions of the wing disk in *Drosophila*. Mol. Gen. Genet. 151, 289–294.

Barnea, E., Sorkin, R., Ziv, T., Beer, I., Admon, A., 2005. Evaluation of prefractionation methods as a preparatory step for multidimensional based chromatography of serum proteins. Proteomics 5, 3367–3375.

Behrens, J., von Kries, J.P., Kuhl, M., Bruhn, L., Wedlich, D., Grosschedl, R., Birchmeier, W., 1996. Functional interaction of beta-catenin with the transcription factor LEF-1. Nature 382, 638–642.

Brennan, K., Gonzalez-Sancho, J.M., Castelo-Soccio, L.A., Howe, L.R., Brown, A.M., 2004. Truncated mutants of the putative Wnt receptor LRP6/Arrow can stabilize beta-catenin independently of Frizzled proteins. Oncogene 23, 4873–4884.

Cadigan, K.M., Fish, M.P., Rulifson, E.J., Nusse, R., 1998. Wingless repression of *Drosophila* frizzled 2 expression shapes the Wingless morphogen gradient in the wing. Cell 93, 767–777.

Campbell, G., Tomlinson, A., 1998. The roles of the homeobox genes aristaless and Distal-less in patterning the legs and wings of *Drosophila*. Development 125, 4483–4493.

Chen, C., Struhl, G., 1999. Wingless transduction by the frizzled and frizzled2 proteins of *Drosophila*. Development 126, 5441–5452.

Cliffe, A., Hamada, F., Bienz, M., 2003. A role of Dishevelled in relocating Axin to the plasma membrane during wingless signaling. Curr. Biol. 13, 960–966.

Cong, F., Schweizer, L., Varmus, H., 2004. Wnt signals across the plasma membrane to activate the beta-catenin pathway by forming oligomers containing its receptors, Frizzled and LRP. Development 131, 5103–5115.

Couso, J.P., Bate, M., Martinez Arias, A., 1993. A Wingless-dependent polar coordinate system in *Drosophila* imaginal discs. Science 259, 484–489.

Couso, J.P., Bishop, S.A., Martinez Arias, A., 1994. The Wingless signalling pathway and the patterning of the wing margin in *Drosophila*. Development 120, 621–636.

Datar, S.A., Jacobs, H.W., de la Cruz, A.F., Lehner, C.F., Edgar, B.A., 2000. The *Drosophila* cyclin D-Cdk4 complex promotes cellular growth. EMBO J. 19, 4543–4554.

Davidson, G., Wu, W., Shen, J., Bilic, J., Fenger, U., Stannek, P., Glinka, A., Niehrs, C., 2005. Casein kinase 1 gamma couples Wnt receptor activation to cytoplasmic signal transduction. Nature 438, 867–872.

Diaz-Benjumea, F.J., Cohen, S.M., 1995. Serrate signals through Notch to establish a Wingless-dependent organizer at the dorsal/ventral compartment boundary of the Drosophila wing. Development 121, 4215–4225.

Dickson, B., Sprenger, F., Hafen, E., 1992. Prepattern in the developing *Drosophila* eye revealed by an activated torso-sevenless chimeric receptor. Genes Dev. 6, 2327–2339.

Dubois, L., Lecourtois, M., Alexandre, C., Hirst, E., Vincent, J.P., 2001. Regulated endocytic routing modulates wingless signaling in *Drosophila* embryos. Cell 105, 613–624.

Duncan, D.M., Burgess, E.A., Duncan, I., 1998. Control of distal antennal identity and tarsal development in *Drosophila* by spineless-aristapedia, a homolog of the mammalian dioxin receptor. Genes Dev. 12, 1290–1303.

Funayama, N., Fagotto, F., McCrea, P., Gumbiner, B.M., 1995. Embryonic axis induction by the armadillo repeat domain of beta-catenin: evidence for intracellular signaling. J. Cell Biol. 128, 959–968.

Hatini, V., DiNardo, S., 2001. Divide and conquer: pattern formation in *Drosophila* embryonic epidermis. Trends Genet. 17, 574–579.

Huppert, S.S., Le, A., Schroeter, E.H., Mumm, J.S., Saxena, M.T., Milner, L.A., Kopan, R., 2000. Embryonic lethality in mice homozygous for a processing-deficient allele of Notch1. Nature 405, 966–970.

Julius, M.A., Schelbert, B., Hsu, W., Fitzpatrick, E., Jho, E., Fagotto, F., Costantini, F., Kitajewski, J., 2000. Domains of Axin and disheveled required for interaction and function in Wnt signaling. Biochem. Biophys. Res. Commun. 276, 1162–1169.

Kelly, O.G., Pinson, K.I., Skarnes, W.C., 2004. The Wnt co-receptors Lrp5 and Lrp6 are essential for gastrulation in mice. Development 131, 2803–2815.

Kennerdell, J.R., Carthew, R.W., 1998. Use of dsRNA-mediated genetic interference to demonstrate that frizzled and frizzled 2 act in the wingless pathway. Cell 95, 1017–1026.

Lee, T., Luo, L., 2001. Mosaic analysis with a repressible cell marker (MARCM) for *Drosophila* neural development. Trends Neurosci. 24, 251–254.

Li, L., Mao, J., Sun, L., Liu, W., Wu, D., 2002. Second cysteine-rich domain of Dickkopf-2 activates canonical Wnt signaling pathway via LRP-6 independently of Dishevelled. J. Biol. Chem. 277, 5977–5981.

Logan, C.Y., Nusse, R., 2004. The Wnt signaling pathway in development and disease. Annu. Rev. Cell Dev. Biol. 20, 781–810.

Mao, J., Wang, J., Liu, B., Pan, W., Farr, G.H., Flynn, C., Yuan, H., Takada, S., Kimelman, D., Li, L., Wu, D., 2001. Low-density lipoprotein receptor-related protein-5 binds to Axin and regulates the canonical Wnt signaling pathway. Mol. Cell 7, 801–809.

Marois, E., Mahmoud, A., Eaton, S., 2006. The endocytic pathway and formation of the Wingless morphogen gradient. Development 133, 307–317.

Milan, M., Diaz-Benjumea, F.J., Cohen, S.M., 1998. Beadex encodes an LMO protein that regulates Apterous LIM-homeodomain activity in *Drosophila* wing development: a model for LMO oncogene function. Genes Dev. 12, 2912–2920.

Nellen, D., Burke, R., Struhl, G., Basler, K., 1996. Direct and long-range action of a DPP morphogen gradient. Cell 85, 357–368.

Neumann, C.J., Cohen, S.M., 1996. Distinct mitogenic and cell fate specification functions of wingless in different regions of the wing. Development 122, 1781–1789.

Neumann, C.J., Cohen, S.M., 1997. Long-range action of Wingless organizes the dorsal–ventral axis of the *Drosophila* wing. Development 124, 871–880.

Nolo, R., Abbott, L.A., Bellen, H.J., 2000. Senseless, a Zn finger transcription factor, is necessary and sufficient for sensory organ development in *Drosophila*. Cell 102, 349–362.

Noordermeer, J., Johnston, P., Rijsewik, F., Nusse, R., Lawrence, P.A., 1992. The consequences of ubiquitous expression of the wingless gene in the *Drosophila* embryo. Development 116, 711–719.

Nüsslein-Volhard, C., Wieschaus, E., 1980. Mutations affecting segment number and polarity in *Drosophila*. Nature 287, 795–801.

Orsulic, S., Peifer, M., 1996. An in vivo structure–function study of Armadillo, the beta-catenin homologue, reveals both separate and overlapping regions of the protein required for cell adhesion and for wingless signaling. J. Cell Biol. 134, 1283–1300.

Pinson, K.I., Brennan, J., Monkley, S., Avery, B.J., Skarnes, W.C., 2000. An LDL-receptor-related protein mediates Wnt signalling in mice. Nature 407, 535–538.

Reya, T., Clevers, H., 2005. Wnt signalling in stem cells and cancer. Nature 434, 843–850.

Ripoll, P., El Messal, M., Laran, E., Simpson, P., 1988. A gradient of affinities for sensory bristles across the wing blade of *Drosophila melanogaster*. Development 103, 757–767.

Rives, A.F., Rochlin, K.M., Wehrli, M., Schwartz, S.L., Dinardo, S., 2006. Endocytic trafficking of Wingless and its receptors, Arrow and DFrizzled-2, in the *Drosophila* wing. Dev. Biol. 293, 268–283.

Schmidt-Ott, U., Technau, G.M., 1992. Expression of en and Wg in the embryonic head and brain of *Drosophila* indicates a refolded band of seven segment remnants. Development 116, 111–125.

Sprenger, F., Nüsslein-Volhard, C., 1992. Torso receptor activity is regulated by a diffusible ligand produced at the extracellular terminal regions of the *Drosophila* egg. Cell 71, 987–1001.

States, D.J., Omenn, G.S., Blackwell, T.W., Fermin, D., Eng, D., Speicher, D.W., Hanash, S.M., 2006. Challenges in deriving high-confidence protein identifications from data gathered by a HUPO plasma proteome collaborative study. Nat. Biotechnol. 24, 333–338.

Strigini, M., Cohen, S.M., 2000. Wingless gradient formation in the *Drosophila* wing. Curr. Biol. 10, 293–300.

Struhl, G., Basler, K., 1993. Organizing activity of wingless protein in *Drosophila*. Cell 72, 527–540.

Tamai, K., Semenov, M., Kato, Y., Spokony, R., Liu, C., Katsuyama, Y., Hess, F., Saint-Jeannet, J.P., He, X., 2000. LDL-receptor-related proteins in Wnt signal transduction. Nature 407, 530–535.

Tao, Q., Yokota, C., Puck, H., Kofron, M., Birsoy, B., Yan, D., Asashima, M., Wylie, C.C., Lin, X., Heasman, J., 2005. Maternal Wnt11 activates the canonical Wnt signaling pathway required for axis formation in *Xenopus* embryos. Cell 120, 857–871.

Tolwinski, N.S., Wehrli, M., Rives, A., Erdeniz, N., DiNardo, S., Wieschaus, E., 2003. Wg/Wnt signal can be transmitted through Arrow/LRP5,6 and Axin independently of Zw3/Gsk3beta activity. Dev. Cell 4, 407–418.

Vachon, G., Cohen, B., Pfeifle, C., McGuffin, M.E., Botas, J., Cohen, S.M., 1992. Homeotic genes of the Bithorax complex repress limb development in the abdomen of the *Drosophila* embryo through the target gene Distal-less. Cell 71, 437–450.

Veeman, M.T., Axelrod, J.D., Moon, R.T., 2003. A second canon. Functions and mechanisms of beta-catenin-independent Wnt signaling. Dev. Cell 5, 367–377.

Wehrli, M., Dougan, S.T., Caldwell, K., O'Keefe, L., Schwartz, S., Vaizel-Ohayon, D., Schejter, E., Tomlinson, A., DiNardo, S., 2000. Arrow encodes an LDL-receptor-related protein essential for Wingless signalling. Nature 407, 527–530.

Werb, Z., Tremble, P.M., Behrendtsen, O., Crowley, E., Damsky, C.H., 1989. Signal transduction through the fibronectin receptor induces collagenase and stromelysin gene expression. J. Cell Biol. 109, 877–889.

White, P., Aberle, H., Vincent, J.P., 1998. Signaling and adhesion activities of mammalian beta-catenin and plakoglobin in *Drosophila*. J. Cell Biol. 140, 183–195.

Wong, H.C., Bourdelas, A., Krauss, A., Lee, H.J., Shao, Y., Wu, D., Mlodzik, M., Shi, D.L., Zheng, J., 2003. Direct binding of the PDZ domain of Dishevelled to a conserved internal sequence in the C-terminal region of Frizzled. Mol. Cell 12, 1251–1260.

Yanagawa, S., Lee, J.S., Haruna, T., Oda, H., Uemura, T., Takeichi, M., Ishimoto, A., 1997. Accumulation of Armadillo induced by Wingless, Dishevelled, and dominant-negative Zeste-White 3 leads to elevated DE-cadherin in *Drosophila* clone 8 wing disc cells. J. Biol. Chem. 272, 25243–25251.

Zecca, M., Basler, K., Struhl, G., 1996. Direct and long-range action of a Wingless morphogen gradient. Cell 87, 833–844.

Zeng, X., Tamai, K., Doble, B., Li, S., Huang, H., Habas, R., Okamura, H., Woodgett, J., He, X., 2005. A dual-kinase mechanism for Wnt co-receptor phosphorylation and activation. Nature 438, 873–877.